International Obsidian Conference 2021

http://arf.berkeley.edu/projects/ioc2021

Please use this document to relay comments / questions to the poster authors:
IOC 2021 Poster Discussion Google Doc Link

2021 Posters

1 What Determines the Chromatic Features of the Obsidian? The Example of Sierra de las Navajas (State of Hidalgo, Mexico). *Paola Donato, Luis Barba, Maria_Caterina Crocco, Mariano Davoli, Rosanna De_Rosa, Sandro Donato, Raffaele Filosa, Giancarlo Niceforo, Alejandro Pastrana, Gino Mirocle Crisci*

2 The Character and Use of Ferguson Wash Obsidian in Eastern Great Basin Prehistory. *Kyle P. Freund, Lucas R. Martindale Johnson, Daron Duke*

3 Morphology and Texture of Microlites in the Baekdusan and Kyushu Obsidian with Implication for the Different Cooling Condition of Rhyolitic Magmas. *Yong-Joo Jwa, Seonbok Yi*

4 The Carpathian Obsidian – Differences between C1, C2, and C3 Types. *Milan Kohút, A Biroň, F. Hrouda (AGICO Inc., Brno, Czech Republic), T. Mikuš,, S. Milovská, J. Šurka*

5 Lithic Raw Materials Procurement Networks in Corsica in the 2nd and 1st Millennia: The I Casteddi Case. *Arthur Leck, Cheyenne Bernier, Bernard Gratuze, Hélène Paolini-Saez, François-Xavier Le Bourdonnec*

6 Obsidian Maritime Interconnections in Early Holocene Eastern Mediterranean. *Theodora Moutsiou*

7 Annadel and Glass Mountain Obsidian Sources in Sonoma County, California. *Robert H. Tykot, Michelle Hughes Markovics*

8 Obsidian and Salt in the Khoy Plain: Uncovering the Early Bronze Age Obsidian Procurement System of the Salt Mine of Tappeh Doozdaghi, North-Western Iran. *Marie Orange, Akbar Abedi, François-Xavier Le Bourdonnec, Afrasiab Garavand, Fatemeh Malekpour, Catherine Marro*

9 Provenance Study of Silicic Stone Tools from Hajdúság (E Hungary) by Using PIXE and PIGE Techniques. *Peter Rozsa, Árpád Csámer, Sándor Tóth, Zita Szikszai, Zsófia Kertész, Ákos Csepregi, Sándor Gönczy, Béla Rácz*

10 Measurement of Magnetic Susceptibility of Obsidian from Shirataki, Hokkaido, Japan, to Identify the Source of Obsidian Tools. *Kyohei Sano*

11 Imports and Outcrops: A Preliminary Characterization of the Baantu Obsidian Quarry, Wolyta, Ethiopia, Using Portable X-Ray Fluorescence. *Benjamin Smith*

What determines the chromatic features of the obsidians? The example of Sierra de las Navajas (State of Hidalgo, Mexico)

P. DONATO[1]; L. BARBA[2]; M.C. CROCCO[3]; M. DAVOLI[1]; R. DE ROSA[1]; S DONATO[3,4]; R. FILOSA[3]; G. NICEFORO[1]; A. PASTRANA [5]; G.M. CRISCI[1]

[1]: DiBEST- Università della Calabria- Italy; [2]: Instituto de Investigaciones Antropológicas, Universidad Nacional Autónoma de México- México; [3]:Dipartimento di Fisica- Università della Calabria- Italy, [4]: INFN Frascati- Italy; [5]: Instituto Nacional de Antropología e Historia- México

Corresponding author: Paola Donato. E-mail: paola.donato@unical.it

INTRODUCTION: Sierra de las Navajas obsidian

Sierra Las Navajas (State of Hidalgo, Mexico) is a peralkaline extinct volcanic center. It was one of the major sources of obsidian in Mesoamerica.

Obsidians from Sierra de las Navajas are unique throughout the world for their **green colour** and **gold/silver hue**. These features, the absence of crystals and the perfect conchoidal fracture, made them intensively exploited in pre-Hispanic times by important cultures to produce artifacts, weapons, jewelry and magic-religious objects.

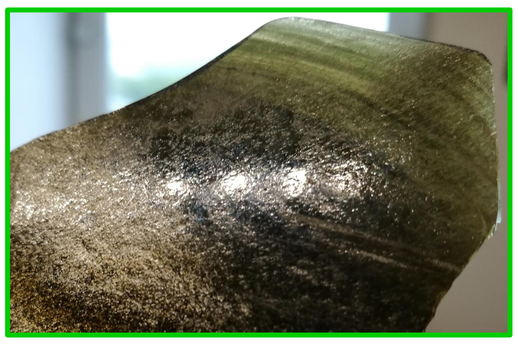

AIM OF THE WORK

To relate their peculiar chromatic features (colour, hue and transparency) to the chemical composition and/or microtexture.

CHEMICAL COMPOSITION AND COLOUR

Microanalysis by Electron Micro-Probe equipped with Wavelength Dispersive Spectroscopy (WDS- EMPA) on different samples revealed that obsidians are **peralkaline.** The comparison with black obsidians from Lipari suggests that the **green colour** of the obsidians is related to a **high iron content**; however, **no significant difference in composition occurs between dark and light green samples, as well as between samples with different hue**.

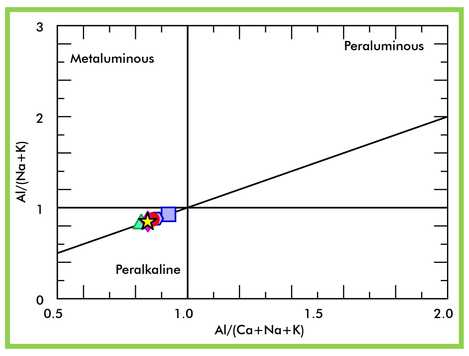

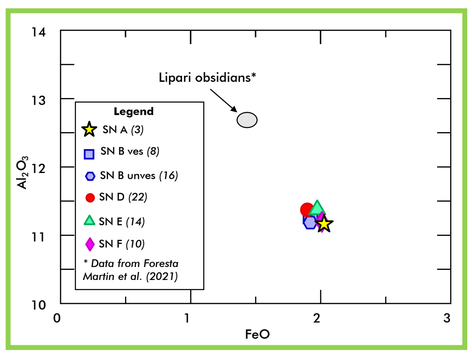

Left: *Maniar and Piccoli (1989) classification of rhyolites;* ***Right:*** *Allumina vs Iron diagram, showing the homogeneous composition of obsidians with different aspect. Black obsidians from Lipari are plotted for comparison.*

Average values are shown. Number in brackets are the number of analysed points.

VESICULATION AND HUE

On samples with different hue we have carried out Scanning Electron Microscope (observation on the surface of the obsidians and X-rays micro-tomographic analyses.

Surface (SEM)
Secundary (SE) and backscattered (BSE) electrons images

Xray- micro-CT
3D distribution of vesicles

Vesicle size
vesicles >10 voxel

V. F vs. E
F: Flatness
E: Elongation

V. Orientation
Polar o.: θ
Azimuthal o.:ϕ

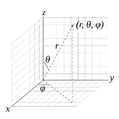

Flatness= 1 –(min.axis/interm. axis)
Elongation= 1 –(interm. axis/major axis)

A

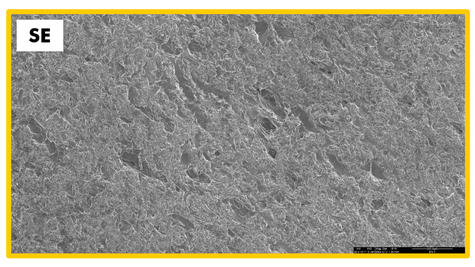

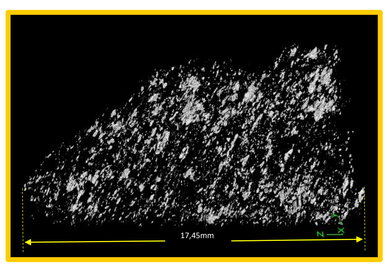

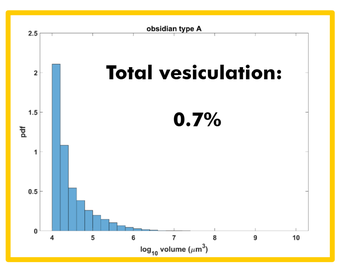

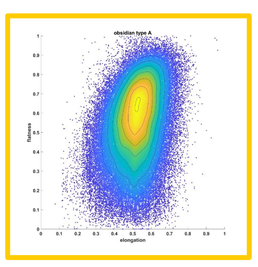

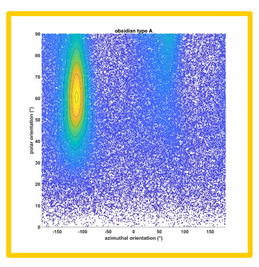

A:
- Unregular surface
- Low vesicularity
- Prevalence of small (ca. 4 μm³) vesicles
- Flat vesicles mainly oriented on preferential planes

B

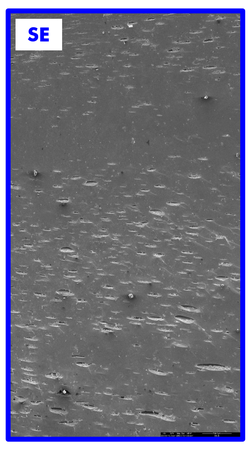

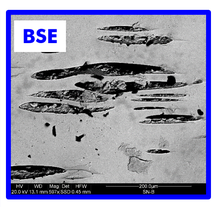

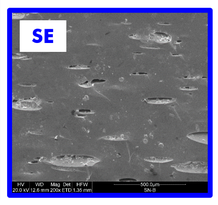

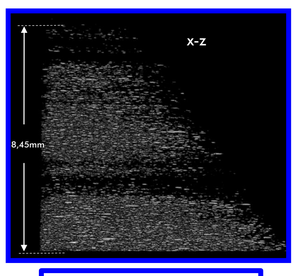

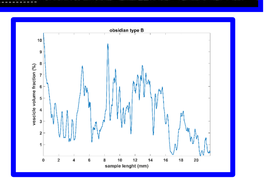

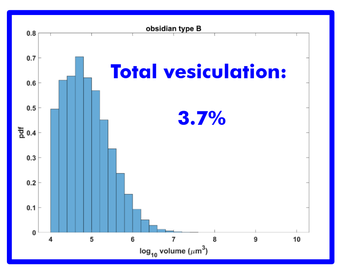

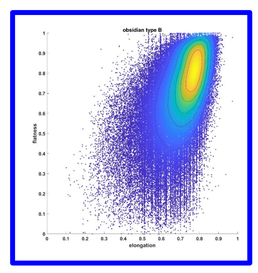

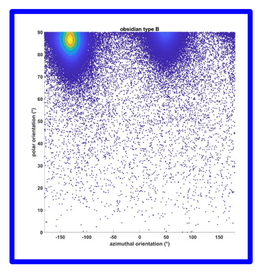

B:
- Rough, vesiculated and smooth, not vesiculated bands
- Large vesicles
- High vesicularity
- Iso-oriented flat and elongated vesicles

D

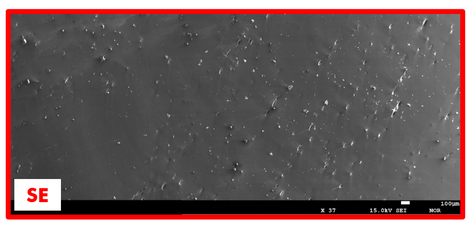

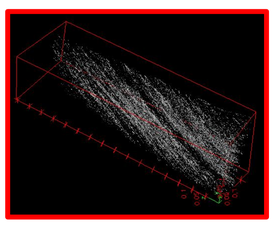

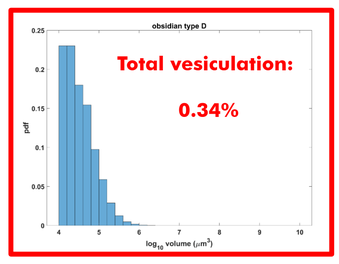

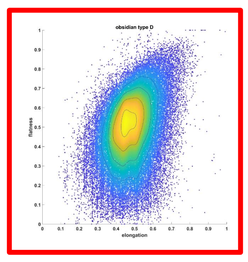

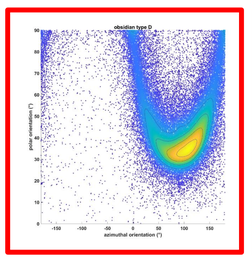

D:
- Smooth surface with thin, vesiculated bands
- Small vesicles
- Very low vesicularity
- Iso-oriented flat and elongated vesicles

E

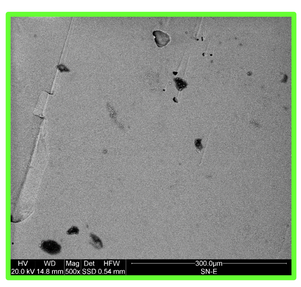

Smooth surface with very few, unregular vesicles

F

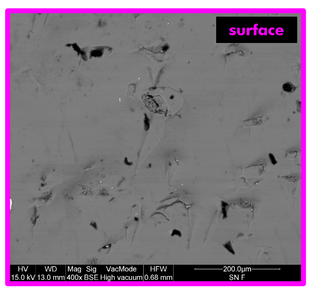

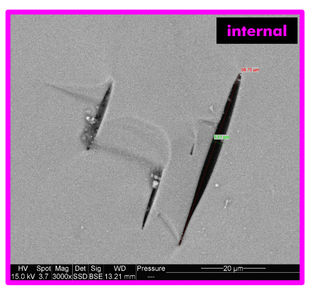

- Very flat, unregular vesicles on the surface
- Few, thin and strongly elongated vesicles inside

SAMPLES

All the analysed samples are from the deposit from which most of the pre-Hispanic obsidians were mined.

Obsidians with different macroscopic aspect were selected for compositional and microtextural studies:

SN A homogeneously green and homogeneous, «metallic» hue

SN B large, concentric bands with different hue and dark to light green colour

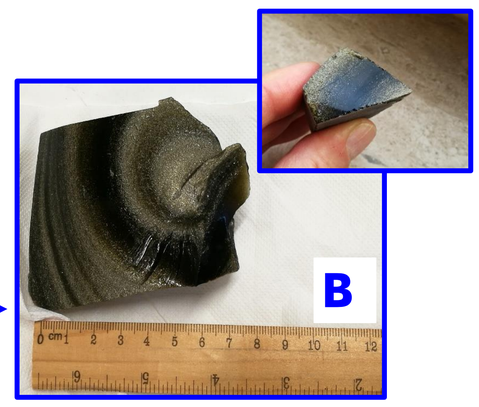

SN D Thin parallel bands with different hue and dark to light green colour

SN E Homogeneous, very dark green, no hue

SN F Homogeneous hue and light green colour on external surface, very dark green, no hue inside

CONCLUSIONS

- The green colour of Sierra de las Navajas obsidians is mainly due to their high Fe content (FeO ca. 2 wt%).
- The amount, shape, dimension and orientation of the vesicles is the main factor controlling the hue and, partly, the colour: non- vesiculated glass has no hue, and the colour appears darker, almost black; on the contrary, the occurrence of vesicles on the surface extols the green colour of the obsidian, making it lighter.
- Transparency is related to the absence of vesicles and microcrystals.

In conclusion, both chemical composition and microvesiculation contribute to determine the chromatic features of Sierra de las Navajas obsidian.

The Character and Use of Ferguson Wash Obsidian in Eastern Great Basin Prehistory

Kyle P. Freund [1, 2] Lucas R. Martindale Johnson [1, 2], and Daron Duke [1, 2]

[1] *Far Western Anthropological Research Group, Inc., Henderson, NV*

[2] *Far Western XRF Laboratory, Henderson, NV*

Introduction

This research characterizes the geology of the Ferguson Wash obsidian source and contextualizes the prehistoric exploitation of its raw materials. The source is located on the Nevada-Utah border in Elko County, roughly 40 kilometers south of the town of Wendover (**Fig. 1**). Prehistoric use of Ferguson Wash obsidian largely begins in the Archaic, being distributed over a relatively small area when compared to other sources in the region.

Ferguson Wash obsidian was first analyzed as part of the Camels Back Cave study (Schmitt & Madsen 2005), but since that time has not been thoroughly characterized. To better understand the geochemistry of the source, 60 geological samples were collected and analyzed using portable X-ray fluorescence (pXRF) spectrometry. The results of this study thus provide a much-needed assessment of the source and its place within the wider framework of eastern Great Basin prehistory.

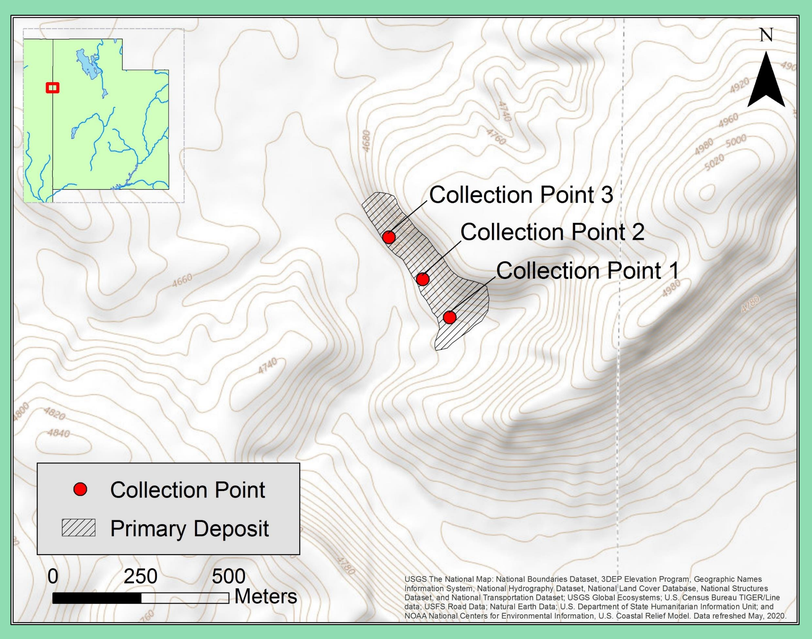

Fig. 1 Map displaying the location of the Ferguson Wash obsidian source and the three points where geological material was collected.

Fig. 2 Primary obsidian deposits from Collection Point 1.

Fig. 3 Northwest facing photograph showing the entrance to the Ferguson Wash canyon (left). Secondary obsidian deposits flowing out of the canyon (right).

Methods

To characterize Ferguson Wash obsidian, 20 samples were collected from three separate localities of primary deposits (**Fig. 1**). All collection points were georeferenced using a handheld Garmin GPS unit and Universal Transverse Mercator (UTM) coordinates.

Samples were analyzed using Far Western's Bruker Tracer III-SD portable XRF instrument set at 40 kV/40 µA for 240 live seconds using a "green" filter composed of 6 mm Cu, 1 mm Ti, and 12 mm Al without a vacuum. Trace-element peak intensities were normalized to the Compton scatter peak of rhodium (19.5–22 keV) and converted to ppm using the MURR 2 matrix-specific calibration. The reference standard USGS RGM-2 was scanned for 90 seconds prior to any new artifact scanning session to confirm the instrument's stability and to provide independent characterization of a known international standard.

To display the results, a bi-variate plot of Y and Rb was produced using ppm measurements, and 95% confidence regions were calculated from the non-Euclidean Mahalanobis Distance statistic using R statistical software (see Johnson et al. 2021).

Results

Estimated to be of Miocene age (Jackson et al. 2009), the primary deposits of Ferguson Wash obsidian extend along a canyon hillside roughly half a kilometer in length. Primary deposits take form within hillside drainage channels in which subangular obsidian pebbles ranging from 1-5 cm in size are embedded within a striated white tephra matrix that also includes pumice (**Fig. 2**). Secondary deposits in the form of rounded and subangular obsidian pebbles can be found in the alluvial channels extending southeast from the canyon's mouth (**Fig. 3**).

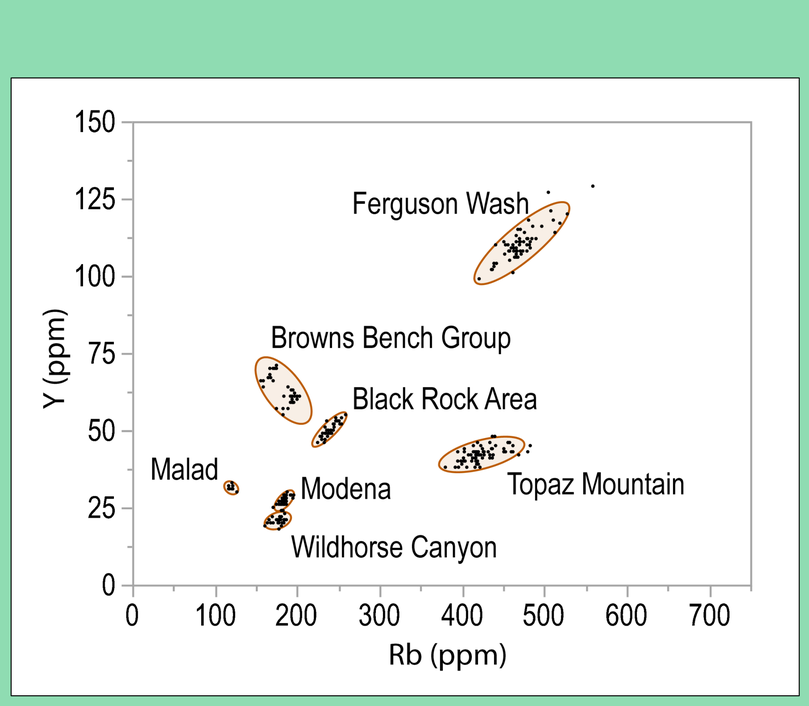

Fig. 4 Bi-variate plot of Y and Rb (in ppm) representing the analyzed samples from Ferguson Wash and other regional obsidian sources.

Through XRF analysis, our study reveals that Ferguson Wash obsidian is chemically distinct from other sources in Utah, Nevada, and Idaho (**Fig. 4**), thus providing the most up-to-date and clearest understanding of the geochemical variability of its raw materials.

Discussion and Conclusions

Ferguson Wash obsidian is present in archaeological assemblages of west-central Utah and east-central Nevada. The diminutive size of its raw materials likely limited their use during the Paleoindian period when larger spearheads and stemmed points were common. This pattern is best demonstrated at the nearby Bonneville Estates Rockshelter, where Ferguson Wash obsidian first appears in the Early Archaic assemblage, primarily taking form as early-stage bifaces (Goebel 2007). Small quantities of Ferguson Wash obsidian are also reported from the Late Archaic assemblage of Mosquito Willies (Young et al. 2008) and at Danger Cave roughly 35 km to the north of the source. Hughes (2014: 216) argues that Danger Cave subsistence practices were more oriented northward, so Ferguson Wash was not a significant part of the lifeways of Danger Cave residents.

Ferguson Wash is a small but interesting part of a much larger pattern of obsidian procurement and exploitation in eastern Great Basin prehistory. We hope this work contributes to elucidating these patterns and provides a foundation for future sourcing work in the region.

References

Goebel, T., A. Holmes, J.L. Keene, & M.M. Coe. 2018. Technological change from the Terminal Pleistocene through Early Holocene in the eastern Great Basin, USA. In *Lithic Technological Organization and Paleoenvironmental Change*, edited by E. Robinson and F. Sellet, pp. 235-261. Springer, Cham, Switzerland.

Hughes, R.E. 2014. Long-term continuity and change in obsidian conveyance at Danger Cave, Utah. In *Archaeology in the Great Basin and Southwest*, edited by N.J. Parezo and J.C. Janetski, pp. 210-225. University of Utah Press, Salt Lake City.

Jackson, R., J. Spidell, D. Kennedy-Spidell & A. Kovak. 2009. *A Historic Context for Native American Procurement of Obsidian in the State of Utah*. Report prepared by Pacific Legacy, Inc. for Logan Simpson Design, Inc., Cameron Park, CA.

Johnson, L.R.M., K.P. Freund, K. Davis, & D. Duke. 2021. Confidence in sourcing small obsidian objects: Applying the Mahalanobis Distance statistic in ternary diagrams with R. Paper presented at the IOC 2021, virtual.

Schmitt, D.N., & D.B. Madsen. 2005. *Camels Back Cave*. University of Utah Anthropological Papers 125. University of Utah Press, Salt Lake City.

Young, D.C., K.L. Carpenter, D. Duke, E. Wohlgemuth, & T. Wriston. 2008. Mosquito Willies (42To137): Prehistoric Data Recovery in Locus 3, Tooele County, UT. Far Western Anthropological Research Group, Inc., Report No. U-05-FF-097m(e). Submitted to Hill AFB and Select Engineering Services, Ogden.

Morphology and texture of microlites in the Baekdusan and Kyushu obsidians with implication for the different cooling condition of rhyolitic magmas

Yong-Joo Jwa[1], Seonbok Yi[2]

[1] Department of Geology, Gyeongsang National University, Jinju 52828, KOREA

[2] Department of Archaeology, Seoul National University, Seoul 08826, KOREA

Introduction

▣ Two provenances for prehistoric obsidian artifacts in Korea

- Mt. Baekdusan and Kyushu (Japan)

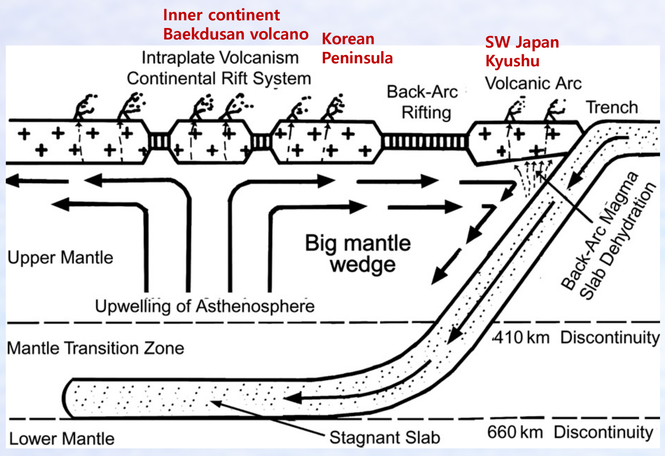

Fig. 2. Tectonic setting in the eastern Eurasian continental margin (Zhao & Liu, 2010)

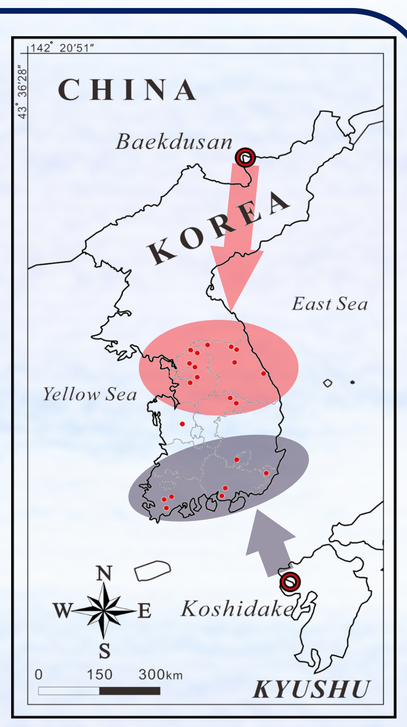

Fig. 1. Two provenances for prehistoric obsidian artifacts in South Korea (Jwa et al., 2019)

▣ Microlites

- tiny crystals (~ 1㎛) included in obsidians
- provide a clue for the cooling condition of rhyolitic magmas

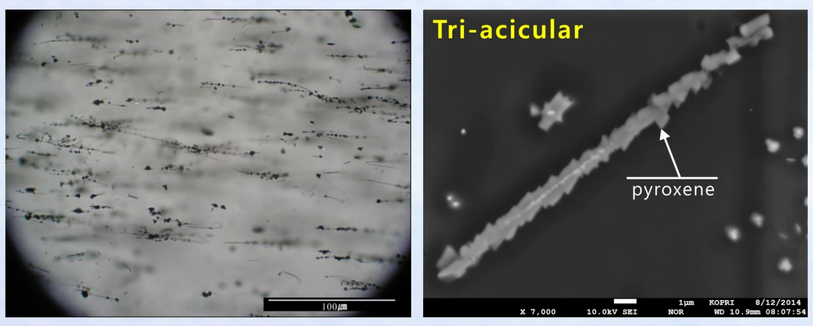

Fig. 3. A microphotograph (left) and a SEM-BSE image (right) of microlites in obsidians

▣ Purpose of this study

- ➢ To compare the morphological and mineralogical characteristics of the Baekdusan and Kyushu obsidians
- ➢ To understand the contrasting mode of crystallization between the Baekdusan and Kyushu obsidians

Analytical Results (1)

▣ Examination of microlite morphology using SEM-BSE

- Since the conventional discrimination of microlites were made from the observation by optical microscopy, it is not easy to identify the actual phase relationship among microlites.
- Morphology and phase relationship between microlites were examined using SEM-BSE.

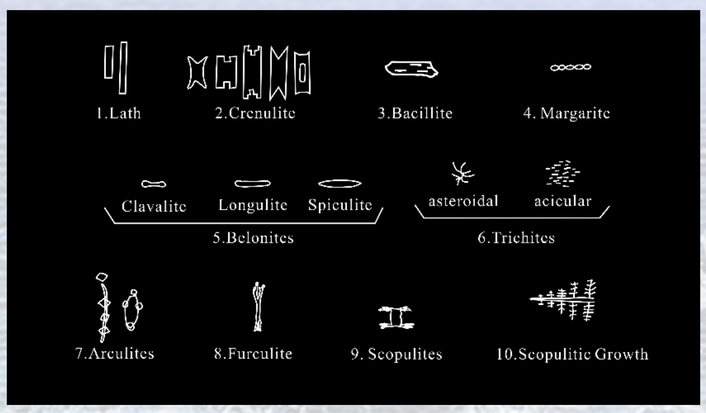

Fig. 4. Morphological discrimination of microlites

Table 1. New description of microlite morphology by SEM-BSE observation

Microlite type	Description from SEM-BSE observation
Lath	Needle-like or prism-like euhedral microlite
Crenulite	Lath-type microlite with corroded edge or core, partly showing skeletal texture
Bacillite	Lath-type microlite with diamond-shaped edges, partly showing spongy cellular texture
Margarite	Lath- or Bacillite-type microlites with one directional swarming of nanolites, partly forming punctuated aggregates
Belonites	Mostly prismatic microlite of single composition: Clavalite of central concave, Longulite of long ellipsoide, and Spiculite of central convex
Trichites	Asteroidal microlites with radial or spiral patterns, and Acicular microlites showing linear aggregates of nanolites regardless of types
Arculites	Long needle-like microlites or stubby-like Belonites, partly showing poikilitic or intergrowth texture
Furculite	Bundle of thin cord with distal ends of diverging to several pieces
Scopulites	Aggregate of Furculite microlites
Scopulitic growth	Growth of Lath or Bacillite microlites showing outward branch-like or feather-like dendritic texture

Analytical Results (2)

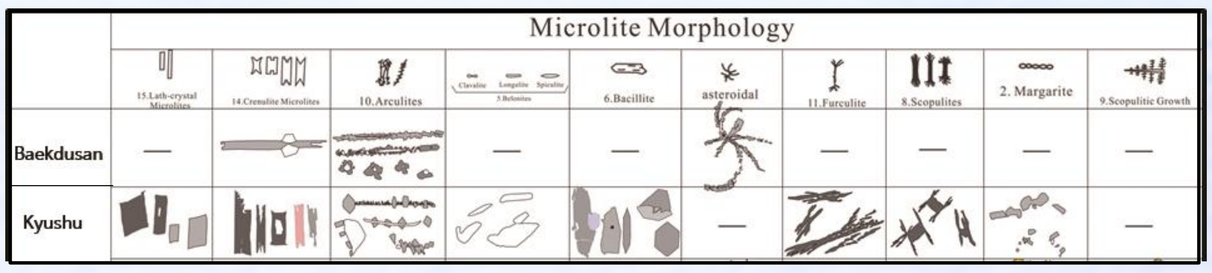

Fig. 5. Morphological characteristics of microlites in the Baekdusan and Kyushu obsidians

Table 2. Contrasting characteristics of microlites between the Baekdusan and Kyushu obsidians

Baekdusan obsidian	characteristics	Kyushu obsidian
acicular, asteroidal, cumulite	microlite morphology	acicular, margarite, lath, asteroidal, crenulite
Fe-oxide, clinopyroxene, alkali feldspar	mineral assemblage	Fe-oxide, clinopyroxene, plagioclase, biotite
Fe-oxide within Cpx (Poikilitic)	microlite paragenesis	Cpx overgrowth around Fe-oxide
augite~hedenbergite	Cpx composition	ferrosilite~pigeonite
sanidine~anorthoclase	Fd composition	oligoclase~andesine

Discussion

▣ Estimation of oxygen fugacity (f_{O2}) during crystallization

at high fo_2

earlier crystallization of Fe-oxides (magnetite or ilmenite)

- poikilitic texture in the Baekdussan obsidian

at medium fo_2

synchronous crystallization of Fe-oxides and silicate minerals

- intergrowth texture in the Kyushu obsidian

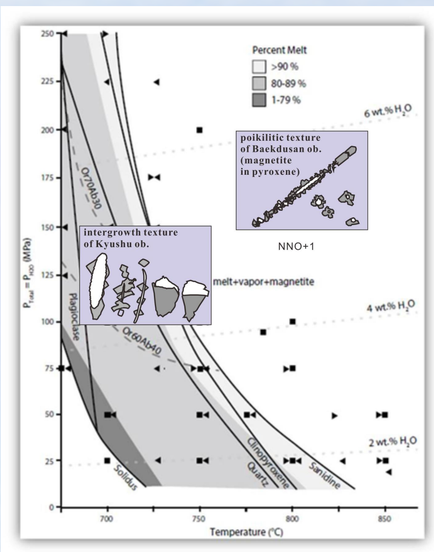

Fig. 6. The crystallization sequence at equivalent water pressure and temperature conditions (Befuss & Gardner, 2016)

▣ Estimation of cooling rate during ascent

at surface

- cooling rate ~1450℃/hr
- almost glassy
- formation of dendritic texture due to rapid cooling

at conduit

- cooling rate ~ 2.5 to 40 ℃/hr
- depth due to size and morphology of microlites
  conduit wall: obsidian / center: bubble and pumice
- formation of skeletal texture in the subsurface or conduit

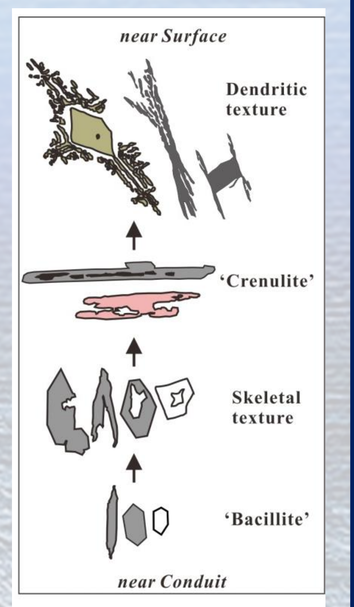

Fig. 7. Typical morphology of microlites according to the relative depth of undercooling magma in the conduit

Conclusion

- When we examine the microlites through a high-resolution scanning electron microscope, they show very distinct mineral assemblage and texture.
- For example, the microlites in the Baekdusan and Kyushu obsidians represent the different textural relationships. Early crystallized Fe-oxides in the Baekdusan obsidians occur within the oikocrysts of clinopyroxene, showing poikilitic texture.
- On the other hand, the clinopyroxene microlites in the Kyushu obdisiands are overgrowing around the Fe-oxides or interlocking with the Fe-oxides.
- This kind of texture between Fe-oxide and clinopyroxene would indicate the differing crystallization process of quenching rhyolitic magma. In general, microlites nucleate during the ascent of rhyolitic magma.
- Judging from the morphology and texture of microlites, the microlites from the Baekdusan obsidians were likely to have nucleated at conduit under high oxygen fugacity, whereas those from the Kyushu obsidians at near conduit and/or surface under medium oxygen fugacity.

The Carpathian obsidians – differences between C1, C2 and C3 types

Milan Kohút[1], Adrián Biroň[1], František Hrouda[2], Stanislava Milovská[1] & Juraj Šurka[1]

[1] - Earth Science Institute, Slovak Academy of Sciences, Bratislava and Banská Bystrica, SLOVAKIA

[2] - AGICO Inc., Brno, CZECH REPUBLIC

IOC 2021
International Obsidian Conference
Berkeley, CA

The Carpathian obsidians: C1 – Zemplín area (SE Slovakia – localities: Brehov, Cejkov, Hraň, Streda nad Bodrogom, and Viničky), C2 – Tokaj region (NE Hungary – localities: Erdőbénye, Lebuj and Mád), and C3 – Zakarpattia province (W Ukraine – locality: Rokosovo 2x) were studied in detail. Present study has been realised by means of Electron Probe Micro-Analysis (EPMA) of glass + minerals, LA ICP MS from glass spots and WR, μCT, X-ray spectroscopy (XRD), Raman spectroscopy, and Magnetic susceptibility + thermomagnetic curves.

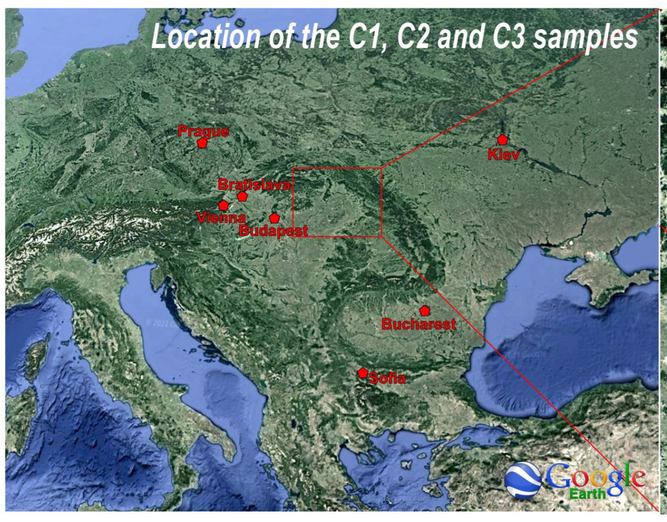

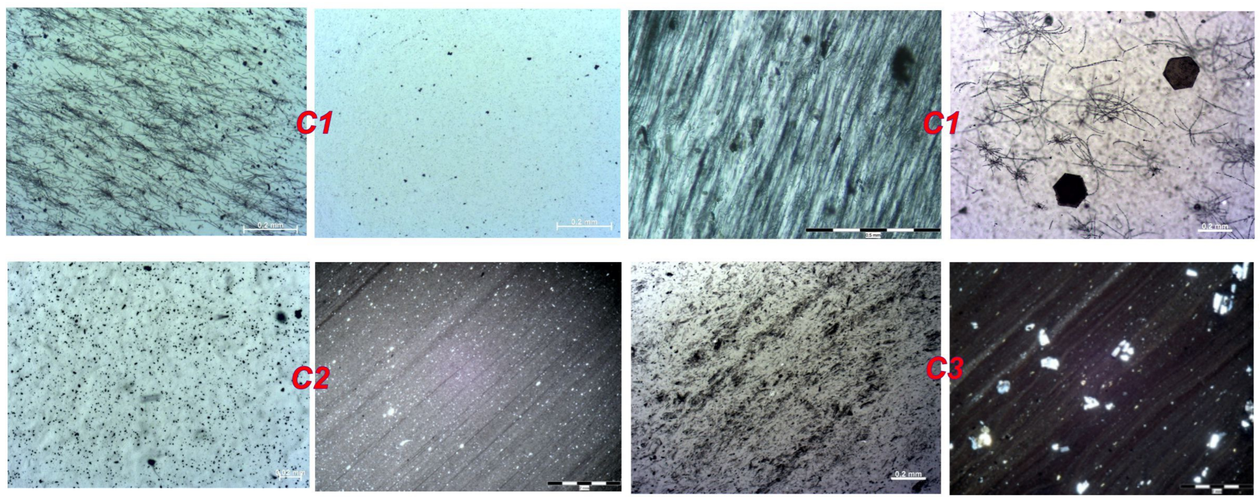

There is no principal difference in character of samples including microscopic view.

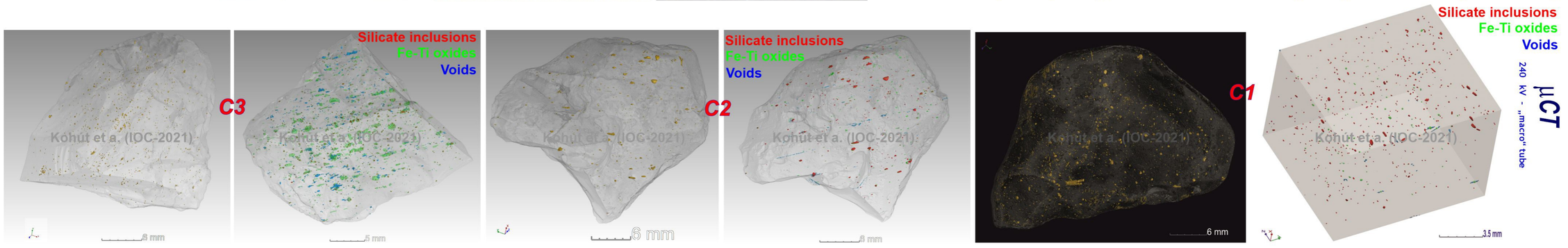

The micro computed tomography (μCT) by dual scanning with the „macro" tube (240 kV) and „micro" tube (180 kV) revealed various presence of the Fe-Ti oxides (hematite, magnetite), silicate minerals (pyroxenes, amphiboles ±olivine) and voids or vesicles. Generally, there was observed domain distribution of these components within all studied samples, nevertheless there are differences between C1, C2 and C3 groups see Table for comparison.

	silicate inclusions	Fe-Ti oxides	voids	total inclusions
C1	0.012 - 0.557	0.003 -0.055	0.001 - 0.009	0.016 - 0.612
C2	0.005 - 0.027	0.019 - 0.038	0.002 - 0.004	0.048 - 0.219
C3	0.015 - 0.266	0.016 - 0.018	0.003 - 0.037	0.033 - 0.321

results in vol. %

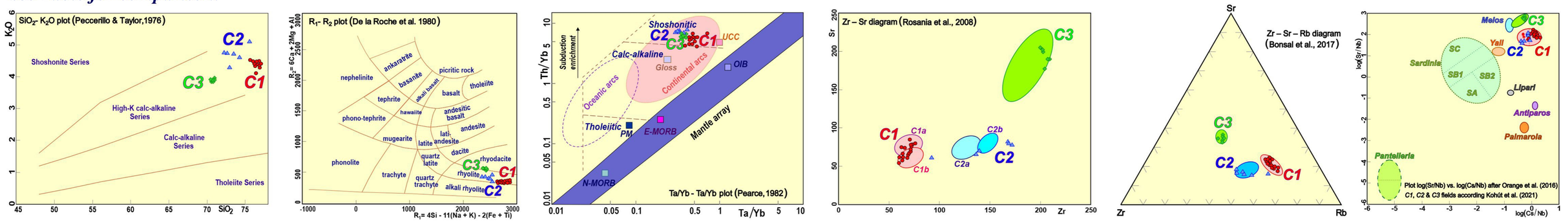

Chemical composition shows significant differences in the major and trace element contents that is obvious in petrogenetic and provenance diagrams - see above.

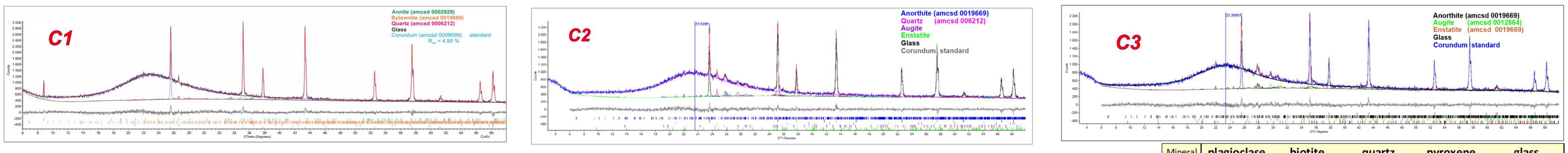

PXRD patterns of representative samples of the Carpathian obsidians. Mineralogical composition obtained by Rietveld Analysis. However, there are differences in the contents of glass and main mineral forms presenting as microlites and/or xenocrysts; see Table for comparison.

Mineral	plagioclase	biotite	quartz	pyroxene	glass
C1	0.31 - 1.22	0.16 - 0.70	0.06 - 0.17	bdl	98.50 - 99.30
C2	0.25 - 1.53	bdl - 0.15	0.36 - 0.65	4.63 - 6.50	92.81 - 93.20
C3	0.33 - 1.80	bdl	bdl	5.54 - 6.08	92.05 - 92.13

results in wt.%

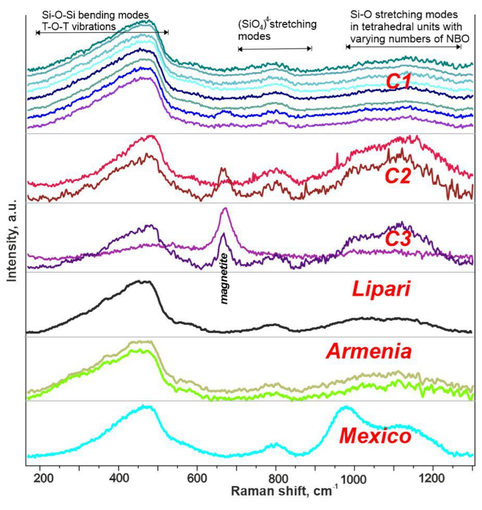

Raman spectroscopy - reflecting composition of glass shows uniform pattern for all studied C1 samples; although the C2 and C3 samples are influenced by magnetite nano-trichites mainly. Generally, there is some similarity to the Palmarola and/or Lipari obsidians.

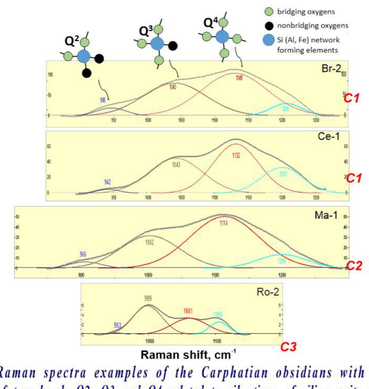

Raman spectra examples of the Carphatian obsidians with complex of tree bands Q2, Q3 and Q4 related to vibrations of silica units with zero, one or two non-bridging oxygens, after substraction of the cubic baseline and deconvolution.

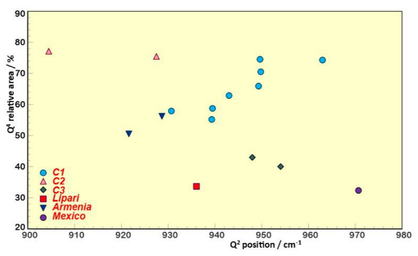

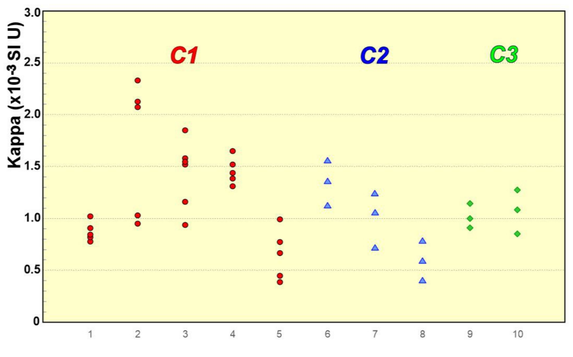

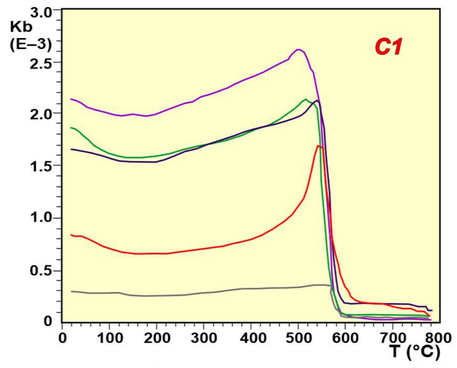

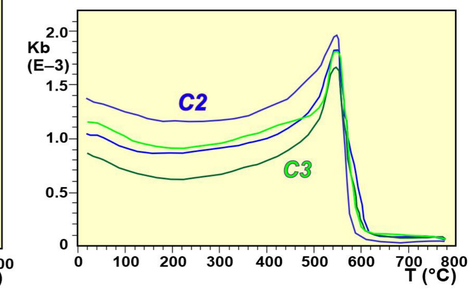

Magnetic Susceptibility The most striking feature is the large drop in susceptibility between 570 and 590 °C, which corresponds to the Curie temperature of magnetite at which ferromagnetic magnetite turns to paramagnetic due to thermal fluctuations (Brown motion). Because of the domain distribution of the ferromagnetic components (magnetite, hematite ±pyrrhotite) significant difference can be within one hand speciment. However, thermomagnetic curves show differences within studied samples and/or C1, C2 and C3 groups.

***Conclusion:** Historically known groups of the Carpathian obsidians (C1, C2 and C3) have been confirmed by a comprehensive study. The basic differences are due to the different chemical composition of glass + WR, and the domain distribution of the main mineral components.*

Lithic Raw Materials Procurement Networks in Corsica in the 2nd and 1st Millennia: The I Casteddi Case

Arthur Leck[1], Cheyenne Bernier[1], Bernard Gratuze[2], Hélène Paolini-Saez[3], François-Xavier Le Bourdonnec[1]

[1]*Université Bordeaux Montaigne, IRAMAT-CRP2A, UMR 5060 CNRS, Pessac, France*
[2]*Université d'Orléans, IRAMAT-CEB, UMR 5060 CNRS, Orléans, France*
[3]*Laboratoire Régional d'Archéologie, Ajaccio, France & Adjunct Research Fellow, Université de Toulouse Jean-Jaurès, TRACES, UMR 5608 CNRS, Toulouse, France*

The I Casteddi site (423 m a.s.l.) is located on the municipality of Tavera, in the Gravona valley, in West-central Corsica. The landscape is one of middle and high mountain, in one of the main transverse valleys linking the Haute-Corse and Corse-du-Sud. I Casteddi is composed of a standing stone (statue-menhir) erected on the Tagliafarro pass and, 300 meters north, a settlement placed on a headland organised in successive terrasses. The excavations led since 2014 have highlighted an oval-shaped dwelling, dated from the Middle Bronze Age and including hearth floors, numerous food macroremains, and domestic objects (Paolini-Saez and Arobba, 2018; Paolini-Saez *et al*., 2021).

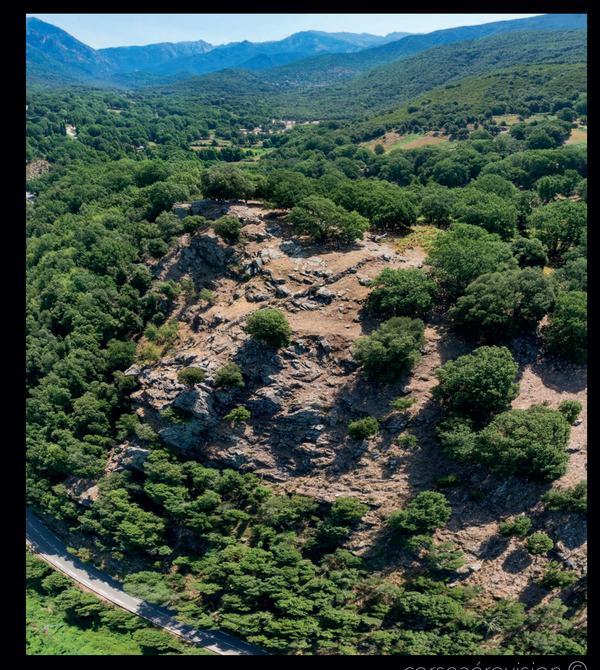

corseaérovision ©

A provenance study on 182 obsidian and 249 rhyolite artefacts was conducted at the IRAMAT following a strictly non-destructive protocol. Among the artefacts analysed, 45% originate from the Middle Bronze Age occupation levels, 15% from the Final Bronze Age, and 35% from the Late Iron Age. These proportions indicate a continuity in the lithic raw material procurement and exploitation on the site. During the Middle Bronze Age, in particular, the artefacts originating from the dwelling refer to domestic contexts linked to food preparation. During the Late Iron Age, they are associated with a floor exhibiting signs of artisanal activities, in the margins of a silo, including metalwork and domestic activities that are yet to be identified.

DRAC-Corse ©

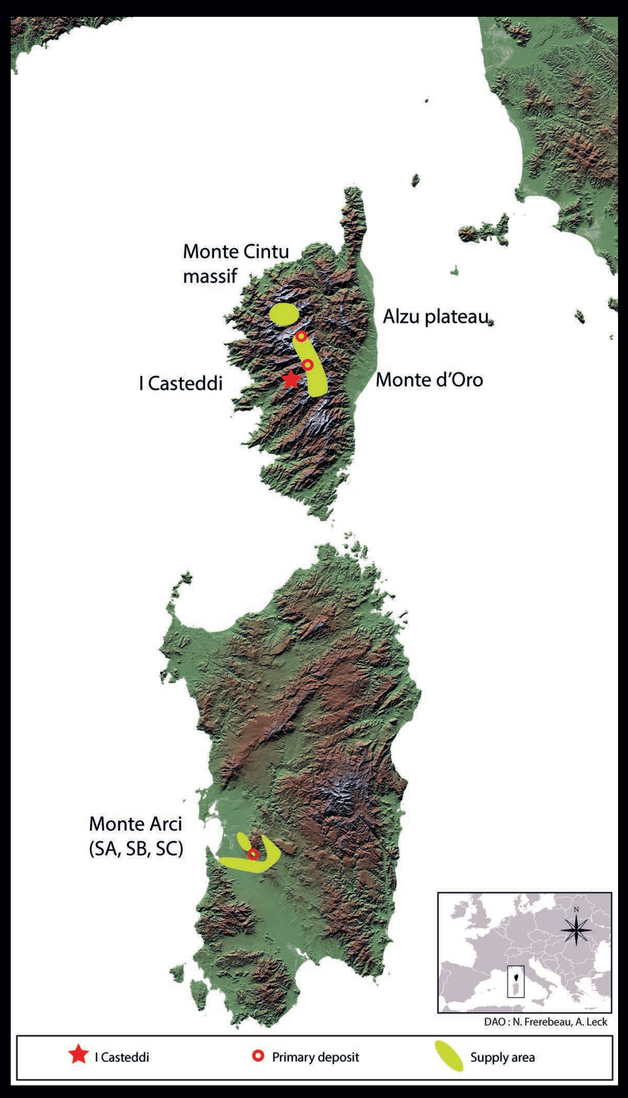

Geochemical analyses were conducted on the obsidian artefacts using EDXRF and LA-ICP-MS (Gratuze, 1999; Orange *et al*., 2017). By comparing the compositional data obtained on the artefacts to those of geological samples from the island-sources of the Mediterranean, we can affirm that the majority of the obsidian found at I Casteddi originates from Sardinia. The SC type greatly predominates (SA: 38, SB1: 1, SB2: 8, SC: 133). Two artefacts remain of unknown origin. These results could attest of a continuity of exchanges within the corso-sardinian bloc.

The geochemical compositions of the rhyolite artefacts were determined by EDXRF (Leck *et al*., 2018) and compared to a geological database constituted of several dozen outcrops sampled in Corsica as well as artefacts already analysed on other sites. The results show that the rhyolites come from a minimum of 25 distinct sources, clustered into 13 visually coherent groups (according to texture, inclusions, colours, and cortex). Although they cannot all be precisely located for the moment, the high diversity of sources exploited reveals the high mobility of this community. The mountains located in the centre of the island, which have a high potential for herding and hunting, seem to be a privileged area of procurement; this is especially the case for the Alzu plateau, which rhyolites were intensely exploited from the final Neolithic onwards.

Obsidian – EDXRF data

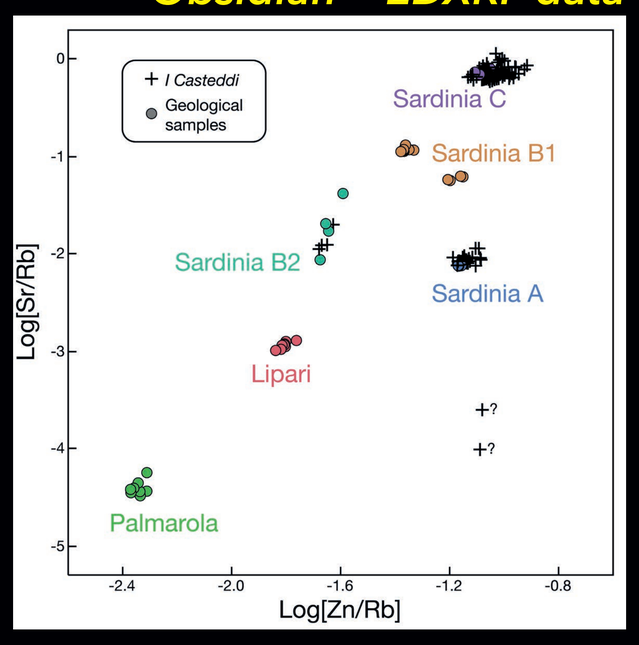

Obsidian – LA-ICP-MS data

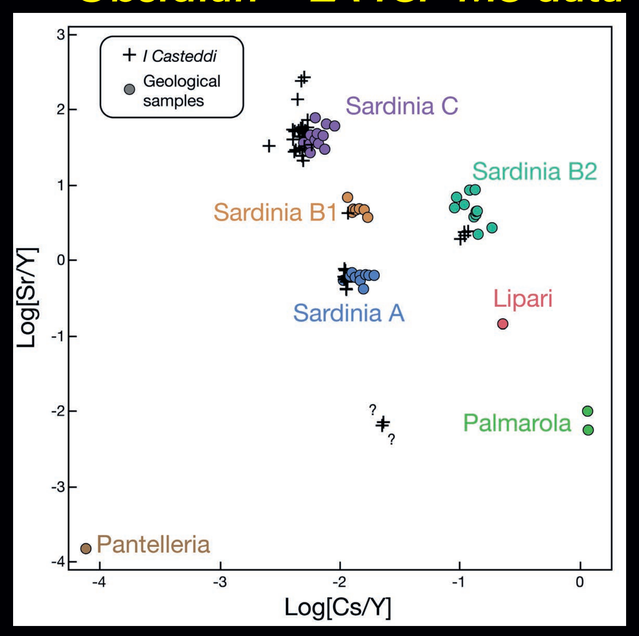

Rhyolite – EDXRF data

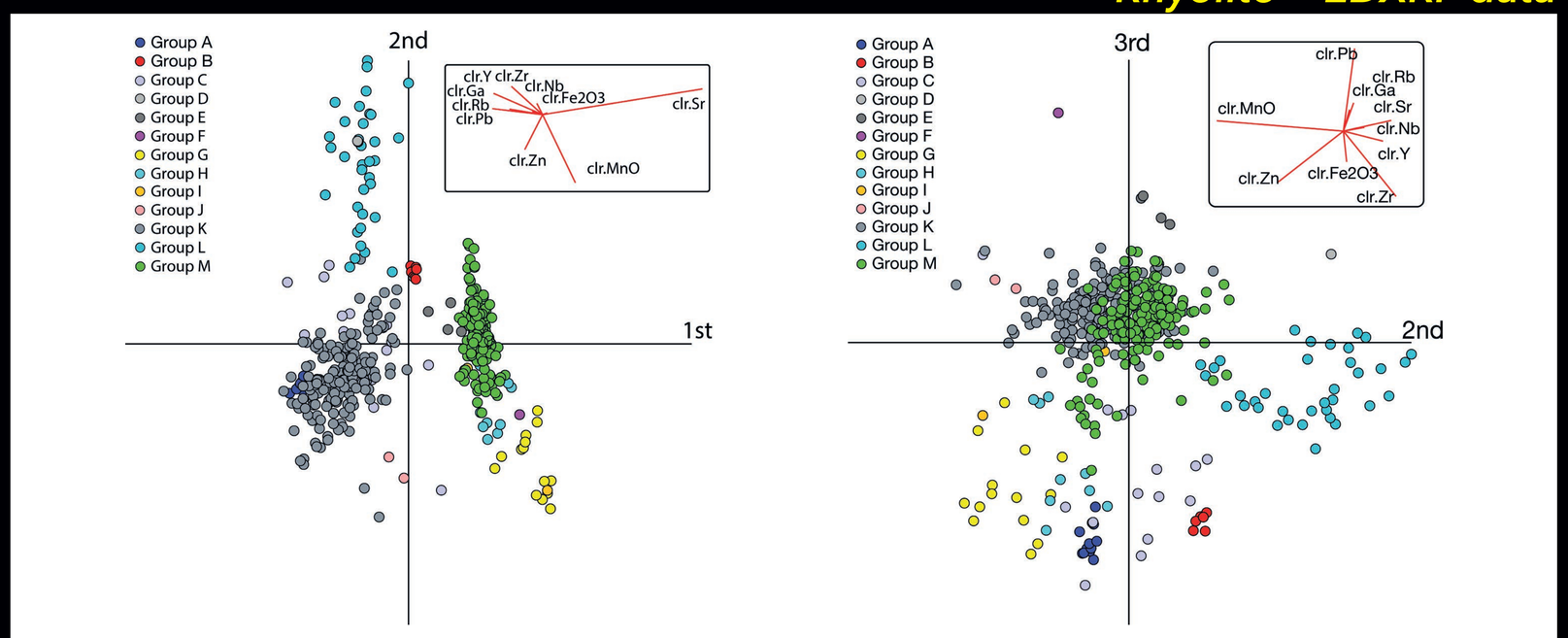

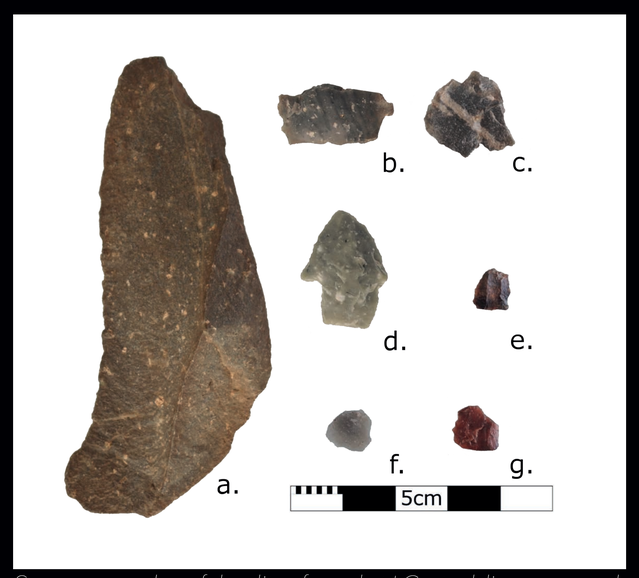

Some examples of rhyolites found at I Casteddi corresponding to groups M (a., b. and d.), K(c.), C(e.), E(f.) and L(g.)

The dichotomy between the lithic procurement patterns – exogenous and therefore maritime for obsidian and allochthonous and mountainous for the rhyolite – is interesting. Do we have two separate and contemporary networks, one linked to long-distance exchanges and the other to the mobility of the group within its territory? Or are those differences chronologically distinct and attest to the changes in the networks of the late Neolithic and Bronze Age? Further studies will have to be conducted to better define the evolution exchange and mobility on the island during the Bronze Age.

References

Gratuze, B., 1999. Obsidian Characterization by Laser Ablation ICP-MS and its Application to Prehistoric Trade in the Mediterranean and the Near East: Sources and Distribution of Obsidian within the Aegean and Anatolia, *J. Archaeol. Sci.* **26**, 869–881.

Leck, A., Le Bourdonnec, F.-X., Gratuze, B., Dubernet, S., Ameziane-Federzoni, N., Bressy-Leandri, C., Chapoulie, R., Mazet, S., Bontempi, J.-M., Marini, N., Remicourt, M., Perrin, T., 2018. Provenance d'artefacts en rhyolite corse : évaluation des méthodes d'analyse géochimique, *C. R. Palevol* **17**, 220-232.

Orange, M., Le Bourdonnec, F.-X., Bellot-Gurlet, L., Lugliè, C., Dubernet, S., Bressy-Leandri, C., Scheffers, A., Joannes-Boyau, R., 2017. On sourcing obsidian assemblages from the Mediterranean area: analytical strategies for their exhaustive geochemical characterisation, *J. Archaeol. Sci. Rep.* **12**, 834–844.

Paolini-Saez, H., Arobba, D., 2018. Etude carpologique du site fortifié d'I Casteddi (Tavera, Corse-du-Sud), *In* Marticorena, P., Ard, V., Hasler, A., Cauliez, J., Gilabert, C., Sénépart, I. (Eds), "Entre deux mers" and Actualité de la Recherche, Proceedings of the XII[e] Rencontres Méridionales de Préhistoire Récente, Bayonne, 29 September – 1 October 2016, Toulouse: Archives d'écologie préhistorique, p. 341–348.

Paolini-Saez, H., Villat, X., Jamai-Chipon, A., 2021. L'occupation protohistorique d'I Casteddi de Tavera (Corse-du-Sud), *In* Six millénaires en Balagne – Sei millenii in Balagne, Balagna, Ghjussani, Ostriconi, Falasorma : archéologie, histoire, architecture et toponymie, Proceedings of the III[e] colloque du Laboratoire régional d'archéologie, Belgodere, 14–16 October 2016, *Cahier Corsica* **281-301**, p.249–264.

Obsidian Maritime Interconnections in Early Holocene Eastern Mediterranean

Theodora Moutsiou[1], Phaedon Kyriakidis[2], Andreas Nikolaidis[2], Georgios Leventis[2], Alexandros Constantinides[2], Evangelos Akylas[2], Constantine Michailides[2], Carole McCartney[1], Stella Demesticha[1], Vasiliki Kassianidou[1], Zomenia Zomeni[3], Daniella Bar-Yosef Mayer[4]

(1) Archaeological Research Unit, University of Cyprus
(2) Department of Civil Engineering and Geomatics, Cyprus University of Technology
(3) Geological Survey Department, Ministry of Agriculture, Rural Development and the Environment of the Republic of Cyprus
(4) The Steinhardt Museum of Natural History, Tel Aviv University

Introduction

Although archaeological evidence has provided a relatively clear picture of when the island of Cyprus was inhabited, there is still considerable debate as to where these inhabitants originated from, as well as the routes they most likely followed to reach the island. Based purely on similarities of the material record, e.g. architecture, lithic technology, fauna, between Cyprus and its surrounding mainland (e.g. Vigne et al. 2011), research has suggested Anatolia and/or the Near East as the original homelands of the first Cypriot settlers (Peltenburg et al. 2001). Obsidian is a common feature of the material culture of the broader region, with material from Anatolian sources traversing the Near East (Figure 1) as far south as Israel (Ibáñez et al. 2015). Obsidian artefacts are also found on the neighbouring island of Cyprus. No geological sources of obsidian occur on the island (Figure 2), which has never been connected to the continent with any form of land bridge. This indicates that obsidian could have only reached Cyprus via seafaring (Moutsiou 2018). Determining the most likely routes for these mainland-island maritime crossings can provide significant information about the Eastern Mediterranean 'socialscape' at the transition from the Pleistocene to the Holocene.

The consumption of obsidian on the island of Cyprus

The island of Cyprus in the Eastern Mediterranean is rich in good quality raw material resources for human exploitation, such as chert, but obsidian is not one of them. Nevertheless exotic obsidian appears in lithic assemblages of Early Holocene (8900-6400 cal BC) sites across the island (Figure 3).Obsidian artefacts are mostly in small quantities (20-50 pieces), although larger assemblages are also known, such as Parekklisia *Shillourokambos* (~600) and Akanthou *Arkosyko* (~5000). Unretouched blades and bladelets dominate the assemblages, formal tools are extremely rare and no evidence for in situ tool manufacture has been unearthed anywhere on the island (Moutsiou 2018). Complete obsidian assemblages were elementally characterised using X-ray Fluorescence Spectrometry (XRF) and demonstrated the dominance of central Anatolian obsidian sources in the Cypriot archaeological assemblages (Figure 4).

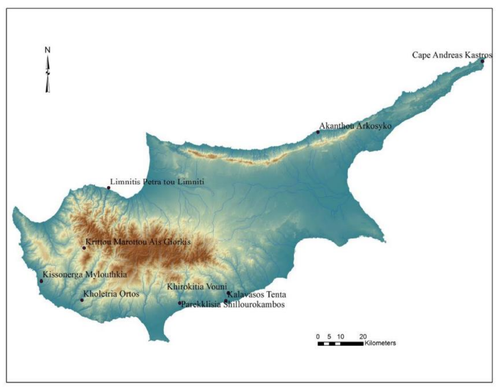

Figure 3. Map showing the main Aceramic Neolithic (8900-6400 cal BC) sites on Cyprus with documented presence of obsidian.

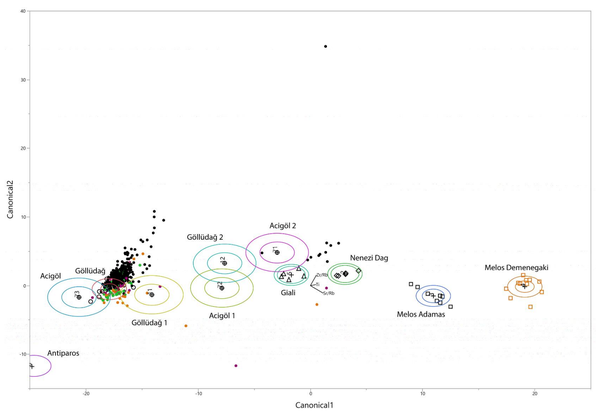

Figure 4. Discriminant Function Analysis (DFA) comparing pXRF data on obsidian from Aceramic Neolithic Cyprus with the main Eastern Mediterranean geological obsidian sources. The figure shows that based on Sr/Rb and Zr/Rb ratios and Ti absolute values, the majority of the Cypriot obsidian can be attributed to the central Anatolian source of Göllü dağ. Colours: black=*Shillourokambos*, green=*Ais Giorkis*, orange=*Mylouthkia*, pink=*Arkosyko* (covered by the *Shillourokambos* main cluster), purle=*Tenta* (Moutsiou 2018).

In Aceramic Neolithic Cyprus, obsidian—when not a surface find—usually derives from contexts that represent everyday activities. Most of the obsidian pieces found across Cyprus (Figure 5) are associated with living floors or fills interior or exterior to building structures. In fact, in all documented instances, there are only two occasions where obsidian artefacts are found within 'special' contexts, although the notion of their association with activities such as feasting or grave goods remains weak. Although the stratigraphic association of obsidian artefacts with domestic rather than religious or other ritual contexts is usually taken to mean that obsidian had no significant value in Aceramic Neolithic Cyprus, it is argued that objects can accrue special value beyond their original functionality, especially when made of materials that are rare, visually distinctive and found at great distances from their source (Saunders 2001, Moutsiou 2018).

Figure 5. Obsidian artefacts from Early Holocene (Aceramic Neolithic) Cyprus.

Obsidian distribution on Cyprus

Least Cost Pathways (LCP) analysis of obsidian distribution across the island (Moutsiou and Agapiou 2019) demonstrates that water played an important role in facilitating obsidian movement on Early Holocene Cyprus. Specifically, our models suggest that (a) riverine and (b) coastal waterways were commonly exploited by the early inhabitants of the island in the context of social exchanges (Figure 6). Moreover, the analysis suggests that not all insular communities were involved in the social landscape delineated by obsidian circulation. The LCP model clearly shows a fragmentation between north and south. A possible explanation could be that in the division between coastal obsidian-bearing sites and inland sites with no obsidian we are, in fact, observing two distinct (contemporaneous but separated) social territories. In this context, the north and south coastlines experience an influx of new populations from the mainland, who settle themselves along the coast as a first stage in the colonization process. During this initial exploration phase, humans are more likely to be risk-averse and obsidian objects would enable the maintenance of social ties as an adaptive strategy in the new conditions.

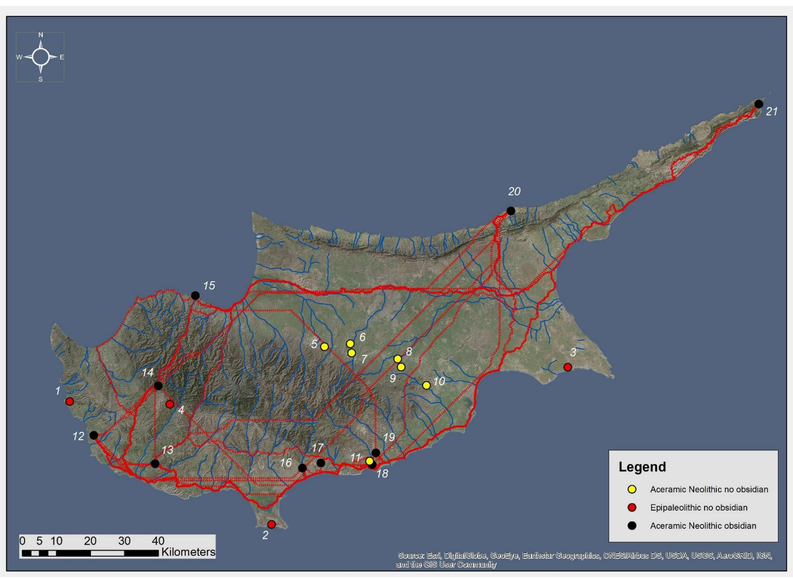

Figure 6. Least Cost Paths Analysis (LCPA) of Aceramic Neolithic sites on Cyprus. The analysis has shown that not all contemporary sites use obsidian. On most occasions sites that do not use obsidian are located at a distance from the least cost routes. However, on some occasions, such as Agrokipia Paleokamina and Pera Chorio Moutti, obsidian is absent from the lithic assemblages even though the sites fall on the least cost route. The image also illustrates that obsidian circulation is fragmented with exploitation restricted along the north and south coasts and a major gap in the interior of the island. Sites: 1=Akamas Aspros, 2=Akrotiri Aetokremmos, 3=Nissi Beach, 4=Vretsia Roudias, 5= Agrokipia Paleokamina, 6=AVA Asprokremmos, 7=Politiko Kelaidoni, 8=Pera Chorio Moutti, 9=Alambra Spileos and Koudourka, 10=Ayia Anna Perivolia, 11=Mari, 12=Kissonerga Mylouthkia, 13=Choletria Ortos, 14=Krittou Marottou Ais Giorkis, 15=Limnitis Petra tou Limniti, 16=Parekklisia Shillourokambos, 17=Ayios Tychonas Klimonas, 18=Kalavasos Tenta, 19=Khirokitia Vouni, 20=Akanthou Arkosyko, 21=Cape Andreas Kastros. [Note: sites 2 and 4=Epipalaeolithic, 1 and 3=Epipalaeolithic?, 5-11=Aceramic Neolithic with no obsidian, 12-20=Aceramic Neolithic with obsidian]. (Moutsiou and Agapiou 2019).

Figure 1. Obsidian distribution in the Near East during the Pre-Pottery Neolithic B (PPNB), 8,500-6,400 cal BC (from Ortega et al. 2016).

Figure 2. Map showing the location of the main geological sources of obsidian in the eastern Mediterranean region neighbouring the island of Cyprus. [Note: 1=Melos, 2=Antiparos, 3=Giali, 4=Sakaeli, 5=Acigöl, 6=Nenezi Dag, 7= Göllüdağ, 8=Erzincan, 9=Ikizdere, 10=Kars, 11=Sarikamis, 12=Erzurum, 13=Bingöl, 14=Mus, 15=Meydan Dag, 16=Suphan Dag, 17=Nemrut Dag, 18=Arteni, 19=Ashotsk, 20=Chikiani]. From Moutsiou 2019.

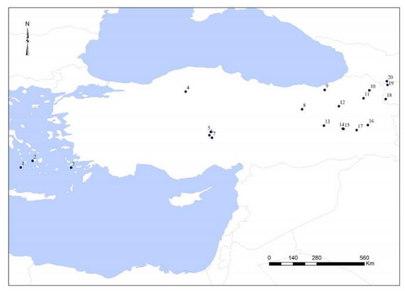

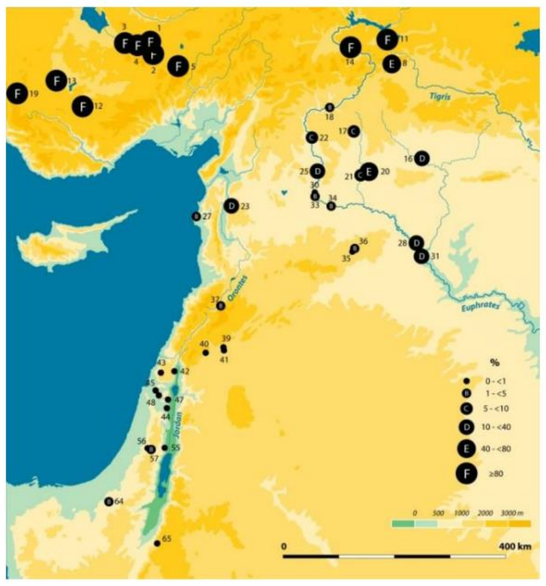

Modeling maritime connectivity in the Eastern Mediterranean

To support archaeological inquiry and inference regarding prehistoric seagoing to/from Cyprus, this project employed Lagrangian-based simulation algorithms for modelling the drift-induced, as well as directed sea-borne movements, based on data and assumptions regarding the prevailing paleo-environmental conditions and vessel characteristics. Although directed seaborne movements are still under investigation, preliminary drift-induced simulation results indicate that there exist at least two periods, during winter for South to North routes (south coast of Anatolia - Cyprus and vice versa), and during summer, for East to West routes (eastern coast of Levant – Cyprus and vice versa), whereby the sea state is favourable to drifting vessels, especially for shorter distances. During almost all the time, departures from the southern side of the Levantine mainland are blocked by currents flowing almost parallel to the coast (Nikolaidis et al. 2020, Figure 7).

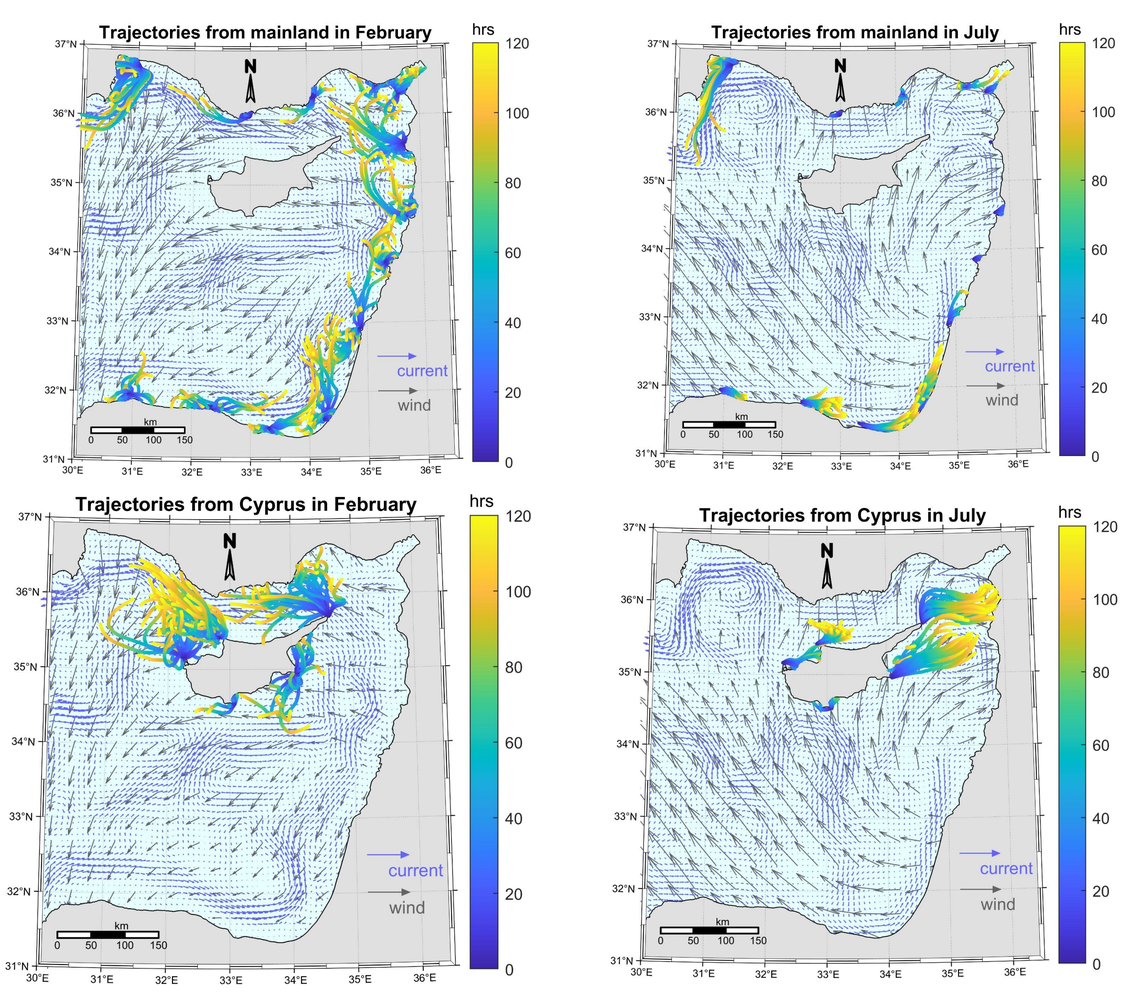

Figure 7. Simulations of prehistoric seagoing to/from Cyprus based on drift-induced modelling (Nikolaidis et al. 2020).

Maritime obsidian networks in the Eastern Mediterranean

The location of Early Holocene obsidian-bearing sites along the north and south coasts of the island and the apparent obsidian gap between the two regions likely support two different mainland routes for the introduction of obsidian to Cyprus: (a) Levant and south coast of Cyprus, and (b) Turkey (Anatolia) and north coast of Cyprus. The application of simulation-based modelling of sea-borne movement in the Eastern Mediterranean allows us to test these hypotheses and determine the most realistic routes for obsidian maritime movement between the island of Cyprus and its surrounding mainland. Work so far points supports both scenarios as likely. The lack of obsidian-bearing sites on the southern coast of Turkey contemporaneous with those found on Cyprus may point towards a closer link with the Levantine mainland.

Conclusions

Complex networks of exchange, where some long distance links between non-neighbouring villages were present (Ortega et al. 2016) in the mainland from the PPNA, with settlements able to develop and maintain distant exchange links that connected different regional exchange networks. The subsequent PPNB period sees an increase in obsidian consumption and longer-distance networks. The detailed analysis of obsidian on Cyprus demonstrates similar patterns were taking place on Cyprus too. The island across the sea was an active participant in this broader 'socialscape' that joined mainland and insular prehistoric communities together. Obsidian exchange (Figure 8), in particular, facilitated the creation and maintenance of long-distance maritime networks. Social networks are a valuable asset crucial for the sharing of information, resources and genes.

Figure 8. Obsidian artefacts from Early Holocene/Aceramic Neolithic Cyprus.

References

Ibañez, J.J., Ortega, D., Campos, D., Khalidi, L., Méndez, V. 2015. Testing complex networks of interaction at the onset of the Near Eastern Neolithic using modelling of obsidian exchange. *Journal of the Royal Society Interface* 12: 20150210
Moutsiou, T. 2019. A compositional study (pXRF) of Early Holocene obsidian assemblages from Cyprus, Eastern Mediterranean. *Open Archaeology* 5(1): 155-166
Moutsiou, T. 2018. The obsidian evidence for trans-maritime interactions in the Eastern Mediterranean: The view from Aceramic Neolithic Cyprus. *Journal of Mediterranean Archaeology* 31(2): 232-251
Moutsiou, T., Agapiou, A. 2019. Least cost pathway analysis of obsidian circulation in Early Holocene–Early Middle Holocene Cyprus. *Journal of Archaeological Science: Reports*, 26. 101881.
Nikolaidis, A., Akylas, E., Michailides, C., Moutsiou, T., Leventis, G., Constantinides, A., McCartney, C. et al. 2020. Modeling drift-induced maritime connectivity between Cyprus and its surrounding coastal areas during early Holocene. *EGU General Assembly Conference Abstracts*, p. 19782.
Ortega D., Ibáñez J.J., Campos D., Khalidi L., Méndez V.,Teira L. 2016. Systems of Interaction between the First Sedentary Villages in the Near East Exposed Using Agent-Based Modelling of Obsidian Exchange. *Systems* 4,18.
Peltenburg, E.J., Colledge, S., Croft, P., Jackson, A., McCartney, C., Murray, M.A. 2001. Neolithic dispersals from the Levantine corridor: a Mediterranean perspective. *Levant* 33: 35-64.
Saunders, N.J. 2001. A dark light: reflections on obsidian in Mesoamerica. *World Archaeology* 33: 220-36.
Vigne, J.-D., Carrère, I. Briois, F., Guilaine, J. 2011. The early process of mammal domestication in the Near East. *Current Anthropology* 52(4): S255-S271.

This work was conducted as part of project SaRoCy, a two- year research project implemented under the "Excellence Hubs" Programme (contract number EXCELLENCE/0198/0143) of the RESTART 2016-2020 Programmes for Research, Technological Development and Innovation administered by the Research and Innovation Foundation of Cyprus. The project's website is https://sarocy.cut.ac.cy

Contact: tmouts01@ucy.ac.cy
UNIVERSITY OF CYPRUS
P.O. Box 20537. CY-1678 Nicosia, CYPRUS
Tel. +357 2289357

Annadel and Glass Mountain Obsidian Sources in Sonoma County, California

Robert H. Tykot[1] & Michelle Hughes Markovics[2]

[1]Department of Anthropology, University of South Florida, Tampa, USA. Email: rtykot@usf.edu; [2]Santa Rosa College, Sonoma, CA.

International Obsidian Conference, April 30 - May 2, 2021

Introduction

Elemental analysis of a collection of prehistoric obsidian artifacts in the Pepperwood Preserve Museum were conducted, followed by a non-systematic survey of two major obsidian sources in the southern North Coast Ranges of California. Specifically, 28 artifacts in the Pepperwood assemblage, from late prehistoric Native American sites in the region, were analyzed non-destructively using a Bruker Tracer III-V+ portable X-ray fluorescence spectrometer, with a filter and time settings emphasizing results for the K-lines energy range of elements Fe through Nb. At least 25 geological samples each from Annadel (in the Sonoma Valley) and from Glass Mountain (Napa Valley) also were analyzed.

Artifacts

Located in the heart of traditional Wappo Indian territory, Pepperwood has an extensive prehistory and history of Native use (Eisemann & Fredrickson 1980). Ethnographic accounts indicate that the Wappo often traveled outside their territory to supplement local resources; e.g. traveling to Lake County to fish (and likely to exploit nearby obsidian sources), to Bodega Bay to exploit marine resources/trade with Pomo and Miwok groups, and to nearby Napa Valley to obtain obsidian from Glass Mountain (Sawyer 1978; Eisemann & Fredrickson 1980). The 28 artifacts analyzed were selected from surface collections in the Pepperwood Preserve, and include formal tools, flakes, cores, and tool fragments.

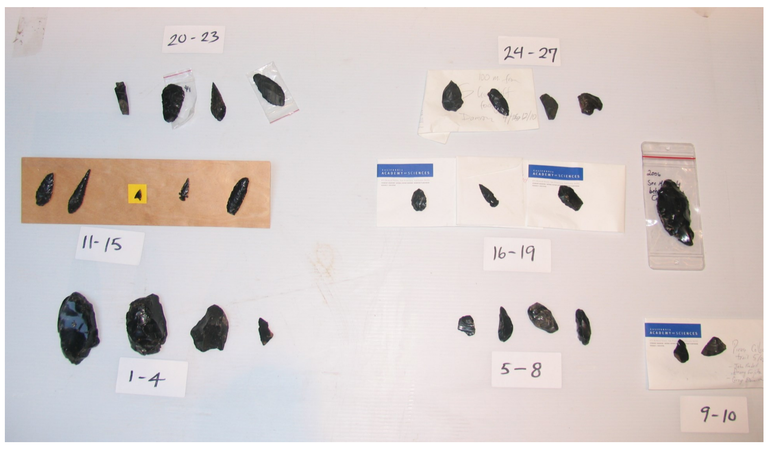

Obsidian artifacts in the Pepperwood Preserve

Potential Sources

There are at least eight known obsidian sources within 100 miles of the Pepperwood Preserve that could potentially be the source of the artifacts tested. These include sources at Borax Lake and Mt. Konocti in Lake County, Mt. Burdell in Marin County, Glass Mountain in Napa Valley, and the Annadel, Franz Valley, Oakmont (Los Guilicos A & B) and Trinity sources in Sonoma County (Silliman 2005). Two major sources were visited, with 29 geological samples collected from nearby Annadel State Park and 25 from Glass Mountain.

Annadel Park

Glass Mountain

Geological samples from Annadel Park (left) and Glass Mountain (right)

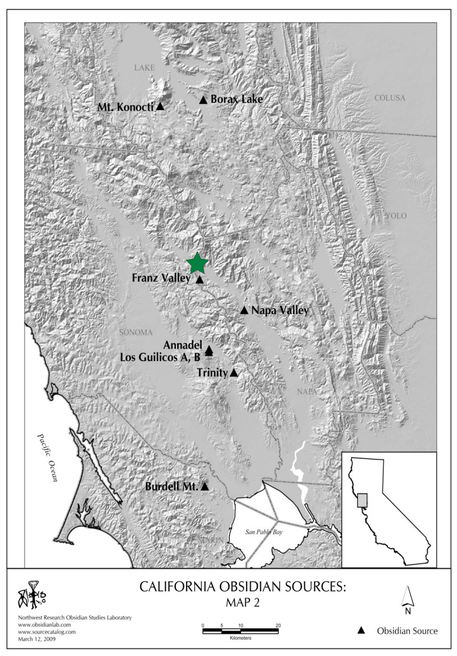

Map showing obsidian sources in northern California. The green star is the Pepperwood Preserve.

Analyses conducted with a Bruker III-V+

Analytical Data for Obsidian Artifacts Tested

Sample	USF #	Fe	Rb	Sr	Y	Zr	Nb	Ba	Th	Source
PW1	14325	10837	140	44	38	219	12	364	12	Annadel
PW2	14326	7590	144	20	28	180	11	331	14	Glass Mountain
PW3	14327	21982	78	101	33	303	17	829	18	?
PW4	14328	7198	135	9	37	195	13	354	12	Glass Mountain
PW5	14329	8240	155	21	32	195	12	262	17	Glass Mountain
PW5b	14329	8037	135	17	38	210	12	192	13	Glass Mountain
PW6	14330	7381	136	10	37	190	10	300	13	Glass Mountain
PW7	14331	7515	146	12	42	214	12	86	13	Glass Mountain
PW8	14332	7034	148	12	35	198	12	224	13	Glass Mountain
PW9	14333	7557	154	12	38	185	12	116	8	Glass Mountain
PW10	14334	11837	134	33	36	205	8	378	11	?
PW11	14335	7822	142	10	43	211	13	202	13	Glass Mountain
PW12	14336	7499	152	15	39	206	14	238	9	Glass Mountain
PW13	14337	10541	130	42	38	227	14	486	14	Annadel
PW14	14338	10309	119	45	37	196	14	307	11	Annadel
PW15	14339	7145	145	17	32	188	12	323	7	Glass Mountain
PW16	14340	7657	148	12	33	182	10	340	13	Glass Mountain
PW17	14341	9093	120	14	35	227	30	637	15	?
PW18	14342	6967	131	11	34	178	11	335	15	Glass Mountain
PW19	14343	11115	138	36	29	207	9	349	11	?
PW20	14344	12033	138	44	28	223	14	517	14	Annadel
PW21	14345	11759	130	46	39	228	13	244	16	Annadel
PW22	14346	6777	151	13	37	193	12	300	16	Glass Mountain
PW23	14347	13021	102	48	42	249	15	605	5	Annadel
PW24	14348	8023	139	19	28	200	11	246	13	Glass Mountain
PW25	14349	8228	139	15	39	192	14	347	9	Glass Mountain
PW26	14350	7775	151	20	29	210	13	209	11	Glass Mountain
PW27	14351	11076	133	47	21	204	9	534	14	?

Methods – pXRF Analysis

Many analytical methods have been used to successfully distinguish between obsidian sources in the Americas. In this study, obsidian artifacts were analyzed using a Bruker III-V+ non-destructive, portable X-ray fluorescence spectrometer. This analytical method has been shown to be very successful on obsidian sourcing (Tykot 2016, 2018, 2021). A specific "obsidian" filter (76 µm Cu, 25 µm Ti, 305 µm Al) was used to enhance results for certain trace elements (Rb, Sr, Y, Zr, Nb) known to be useful for sourcing, while the analysis settings chosen were 40 kV, 10 µA, and 180 seconds. The results were calibrated using a 2008 Excel program with obsidian standards from the University of Missouri Columbia, analyzed by INAA, LA-ICP-MS, and XRF.

Results

An X-Y graph of Rb/Nb vs. Sr/Nb provides a clear distinction between the Annadel State Park and Glass Mountain geological obsidian samples. Sixty percent of the artifacts from Pepperwood were assigned to Glass Mountain, and twenty-one percent to Annadel. Five other artifacts did not match with either and represent at least three other geological sources. A total of twelve sources have been identified in this region, with notable differences in their quality, physical appearance, and selection for producing stone tools (Jackson 1989).

Summary for Geological Samples

Anadel								
no. = 29	**Fe**	**Rb**	**Sr**	**Y**	**Zr**	**Nb**	**Ba**	**Th**
ave	12262	106	44	39	229	12	490	9
std	342	4	2	2	6	1	29	1
min	11770	100	38	36	218	10	438	7
max	13087	113	49	43	241	15	553	11
Glass Mountain								
no. = 25	**Fe**	**Rb**	**Sr**	**Y**	**Zr**	**Nb**	**Ba**	**Th**
ave	7150	143	12	35	194	12	289	13
std	393	7	1	2	11	1	57	1
min	6191	127	11	31	175	11	202	10
max	8066	155	13	40	223	14	425	15

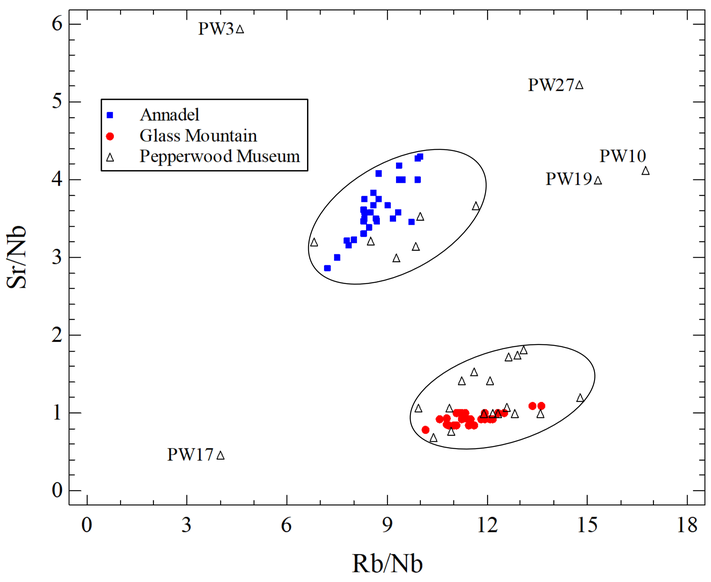

X-Y Graph showing Annadel and Glass Mountain geological samples, and Pepperwood Preserve artifacts

Comparison of the calibrated pXRF data and trace element ratios with analytical data from other studies will be used to suggest what other sources are represented by these outliers; comparison of data from different analytical methods and calibration software is not straightforward.

Conclusions

Our results discriminate among the different sources in northern California, and allow us to attribute archaeological artifacts to them, and address issues about obsidian procurement, trade and usage in this region. This pilot study complements the small number of other studies done and with further work we hope to enhance current understanding of Native American lifeways in this region.

The overall results will be compared with other research on trade and exchange of obsidian in this region of California.

References

California Obsidian Source Index. Northwest Research Obsidian Studies Source Catalog. http://sourcecatalog.com/ca/s_ca.html.

Eisemann, Lynn, and David Fredrickson (1980) Archaeological Investigations at CA-SON-1208 Located in the Franz Valley Area of Sonoma County, California. Cultural Resources Facility at Sonoma State University.

Jackson, T. L. (1989). Late prehistoric obsidian production and exchange in the North Coast Ranges, California. *Contributions of the Archaeological Research Facility* 48: 79-94.

Obsidian Source Maps: United States. Northwest Research Obsidian Studies Laboratory. http://www.obsidianlab.com/image_maps/image_maps.html#ca.

Sawyer, Jesse O. (1978) Wappo. In *Handbook of North American Indians: California* 8:256–263.

Silliman, Stephen W. (2005) Obsidian Studies and the Archaeology of 19th-Century California. *Journal of Field Archaeology* 30(1):75–94.

Tykot, R.H. 2016. Using Non-Destructive Portable X-Ray Fluorescence Spectrometers on Stone, Ceramics, Metals, and Other Materials in Museums: Advantages and Limitations. *Applied Spectroscopy* 70(1): 42-56.

Tykot, R.H. Portable X-Ray Fluorescence Spectrometry (pXRF). 2018. In S.L. López Varela (ed.), *The SAS Encyclopedia of Archaeological Sciences*, pp. 1-5. John Wiley & Sons, Inc.

Tykot, R.H. 2021. Obsidian in Prehistory. In P. Richet (ed.), *Encyclopedia of Glass Science, Technology, History, and Culture*. John Wiley & Sons, Inc.

Acknowledgments

Thanks to Benjamin Benson from the Pepperwood Preserve for providing access to their collections.

OBSIDIAN AND SALT IN THE KHOY PLAIN
UNCOVERING THE EARLY BRONZE AGE OBSIDIAN PROCUREMENT SYSTEM OF THE SALT MINE OF TAPPEH DOOZDAGHI, NORTHWESTERN IRAN

Marie Orange[1,2,3,4], Akbar Abedi[5], François-Xavier Le Bourdonnec[2], Afrasiab Garavand[6], Fatemeh Malekpour[7], Catherine Marro[3]

[1]Archaeology and Palaeoanthropology, School of Humanities, Arts and Social Sciences, University of New England, Australia; [2]IRAMAT-CRP2A CNRS UMR 5060, Université Bordeaux Montaigne, France; [3]Archéorient—Environnements et Sociétés de l'Orient Ancien CNRS UMR 5133, Maison de l'Orient et de la Méditerranée, France; [4]Southern Cross GeoScience, Southern Cross University, Australia; [5]Department of Archaeology and Archaeometry, Tabriz Islamic Art University, Iran; [6]Mohaghegh Aradabili University, Iran; [7]West Azerbaijan Cultural Heritage, Tourism and Handicraft Organisation, Iran

TAPPEH DOOZDAGHI

- Salt mine located in the Khoy plain, Northwestern Iran
- 16 hectares, culminates at c. 24 meters above the surrounding landscape
- First excavation campaign in 2016
- Late Neolithic to Iron Age occupation
- High concentration of Early Bronze Age material culture remains (c. 3500-2400 BCE)

MATERIALS & METHODS

Materials

- 40 obsidian artefacts were retrieved from the Early Bronze Age occupation level; they were all analysed by portable XRF.

Methods

- Instrument: Bruker Tracer III-SD
- Calibration: MURR obsidian calibration
- Elements measured: Mn, Fe, Zn, Ga, Th, Rb, Sr, Y, Zr, Nb
- Measurement specifications: 180 seconds, 40 Kv, 39 µA, green filter (0.006" Cu, 0.001" Ti, 0.012 Al)
- Standards: Several standards were analysed at the beginning and end of each run to ensure the repeatability, accuracy, and precision of our measurements.

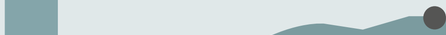

OBSIDIAN PROCUREMENT

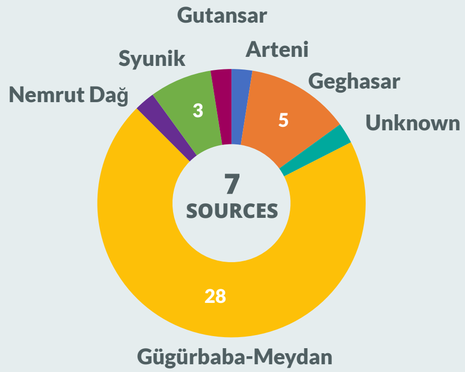

- High diversity of obsidian sources exploited (7 in total) from Eastern Anatolia (72.5%) and the Southern Caucasus (25%).

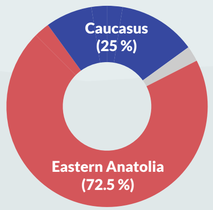

DISCUSSION

- The 40 obsidian artefacts from the Early Bronze Age levels of Tappeh Doozdaghi come from seven different sources located in both Eastern Anatolia and the Southern Caucasus.
- High obsidian procurement diversity suggests that the Khoy plain attracted populations from varied horizons during the Early Bronze Age. They were likely drawn by the numerous natural resources available in the Khoy plain, such as arable land, winter pasturelands, abundant water sources, and salt.
- Similar obsidian sources diversity is also observed on the salt mine of Duzdagi, in Nakhhivan (>90 km North), where both ceramic and obsidian assemblages hint at a possible role of 'pastoralist hub' during the Kura-Araxes period.
- Highlights the key role of local resources (e.g. salt) in the larger circulation system of other staples (e.g. obsidian) and in creating economic and social hubs for populations at the regional and interegional level.

Early Bronze Age ceramics from Tappeh Doozdaghi
©A. Abedi

Provenance Study of Silicic Stone Tools from Hajdúság (E Hungary) by Using PIXE and PIGE Techniques.

Péter Rózsa[1], Árpád Csámer[1], Sándor Tóth[1], Zita Szikszai[2], Zsófia Kertész[2], Ákos Csepregi[2], Sándor Gönczy[3], Béla Rácz[3]

[1]Department of Mineralogy and Geology, University of Debrecen, Debrecen, Hungary
[2]Institute for Nuclear Research (ATOMKI), Laboratory for Heritage Science, Debrecen, Hungary
[3]Ferenc Rákóczi II Transcarpathian Hungarian Collage of Higher Education, Beregovo, Ukraine

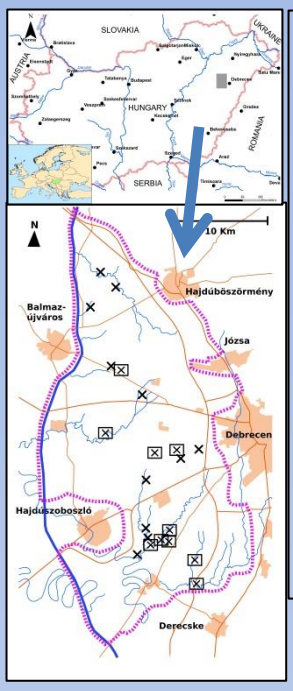

The loessy area of the Hajdúság and Hajdúhát micro-regions (Hajdú-Bihar County, East Hungary) have been inhabited from the Paleolithic. During pilot field-surveys seventeen pieces of chipped silicic stone tools were collected from 21 non-excavated registered archaeological sites located in the southern part of these micro-regions (Fig. 1). The collection area of approximately 560 square km is dominantly agricultural field, and the findings could be collected directly from the surface of the arable land. Seven obsidian findings and ten tools made of other (hydrothermal or limnic) silicic raw material were analyzed. Major and trace element composition of the stone tools were analyzed by Particle Induced X-ray Emission (PIXE) and Proton Induced Gamma-ray Emission (PIGE) techniques. The detected element spectrum includes alkali metals (Li, Na, K, Rb), alkali earth metals (Mg, Ca, Sr, Ba), metals (Al, Ti, V, Cr, Mn, Fe, Co, Ni, Cu, Zn, Ga, Y, Zr, Nb, Hf, Pb), metalloids (B, Si, Ge, As), non-metals (P, S, Se), halogens (F, Cl, Br), as well as lanthanides and actinides (Ce, Th, U), too, although detected concentrations less than 100 ppm have low accuracy. Silica concentrations of the obsidian samples range between 72 and 78%, and, in general, they can be characterized by relatively high Sr, Ba, and Cl content.

Fig. 1. Location of findings (cross: site of sample; cross in square: site of analyzed sample)

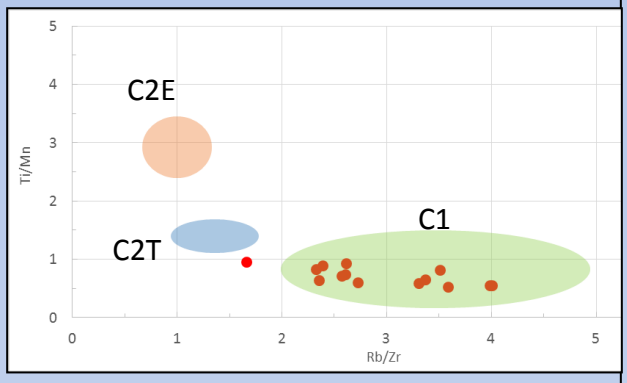

Fig. 2. Ti/Mn vs Rb/Zr diagram

For Transylvanian obsidian tools Ti/Mn vs Rb/Zr binary diagram was used as provenance fingerprint (Constantinescu et al. 2002). As the Transylvanian findings, most of our samples belong to the field of C1 (Slovakian) type; there is only one sample which can be C2T type, i.e. may originate from the Hungarian part of the Tokaj Mountains (Fig. 2).

The hydrothermal and limnic silicic material has more than 98% SiO2 content. Beside silica, quantity of Al2O3 (less than 1%) as well as Na, Mg P, K, Ca (some hundreds ppm) can be detected. In some samples some hundreds ppm of chlorine was analyzed. Presumably, sources of raw material of these tools could be traced in the Tokaj Mountains.

Reference

Constantinescu, B., Bugoi, R., Sziki, G. 2002: Obsidian provenance studies of Transylvania's Neolithic tools using PIXE, micro-PIXE and XRF. Nucl. Inst. Meth. 189. 1-4. 373-377.

Acknowledgement

Financial support by the Access to Research Infrastructures activity in the Horizon 2020 Programme of the EU (IPERION CH Grant Agreement n. 654028) is gratefully acknowledged.

Poster 8

Measurement of Magnetic Susceptibility of Obsidian from Shirataki, Hokkaido, Japan, to Identify the Source of Obsidian Tools

○Kyohei SANO (Graduate School of Regional Resource Management, University of Hyogo)

Research paper information!!
This study is now published in Journal of Regional Resource Management,1,35-43
https://u-hyogo.repo.nii.ac.jp/?action=pages_view_main&active_action=repository_view_main_item_detail&item_id=6238&item_no=1&page_id=13&block_id=46

Introduction

Magnetic susceptibility is often used to identify the source of tools and tombstones that are made from igneous rocks, such as obsidian and granite. This study reports on how the relationship between magnetic susceptibility and sample thickness of obsidian contributes to identifying the source of obsidian tools. Obsidian samples from Shirataki, Hokkaido, Japan, were analyzed, focusing on those from the lava flows of Tokachi-Ishizawa (TI), Akaishiyama (AK), and Horoka-Yubetsu (HY).

Results revealed that obsidian from the HY lava demonstrated the highest value of magnetic susceptibility among the analyzed samples; thus, obsidian from the HY lava could be identified by this characteristic. Concurrently, heterogeneity in the magnetic susceptibility within a single lava flow was observed in the AK lava. These results could contribute to the identification of the source of obsidian tools and development of non-destructive techniques for measurement of magnetic susceptibility.

Geological Setting and Samples

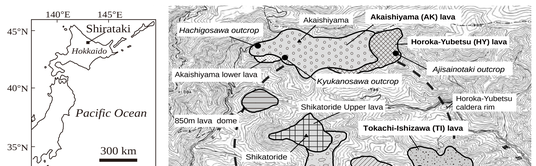

Fig. 1. Distribution map of the obsidian lava flows in Shirataki, Hokkaido, Japan. This map is compiled from Wada and Sano (2011) and Wada and Sano (2016). This map is based on the topo- graphic map published by the Geospatial Information Authority of Japan.

Erupted age

The age of obsidian lava flows in the Shirataki area have been estimated by K–Ar dating as follows: circa 2.24 Ma (± 0.05) for the AK lava, circa 2.26 Ma (± 0.07) for the HY lava, circa 2.20 Ma (± 0.11) for the TI lava, and circa 2.11 Ma (± 0.05) for the Shikatoride lower lava (Wada and Sano, 2011).

Rock texture

Obsidian from TI lava is aphyric and mainly consists of glass (>97 vol.%). Further, it contains microphenocrysts of magnetite (0.05–0.1 mm), microlites of plagioclase (<0.2 mm), oxides (<0.05 mm), rare K-feldspar (<0.05 mm), rare biotite (<0.01 mm), and plagioclase phenocrysts (0.4–1.0 mm) (Sano et al., 2015). The volume fraction of rare crystals is less than 1 vol.%. Obsidians from the AK and HY lavas are composed of mostly glass (>98 vol.%) and microphenocrysts and microlites of magnetite (< 0.07 mm) (Wada and Sano, 2011).

Fig. 2 Photos of the TI (a) and AK (b and c) lava flows.

Analytical method

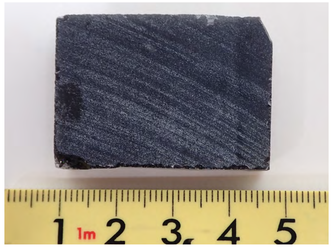

I constructed an obsidian wafer for the measurement of magnetic susceptibility. First, I cut the samples with a rock cutter to create wafers of different thicknesses, ranging from 2.05 to 23.28 mm . The length, width, and area of the wafers range from 28.4 to 38.3 mm, from 22.2 to 34.0 mm, and from 724.2 to 1302.2 mm^2respectively.

Thereafter, I measured the magnetic susceptibility by using the KT-10v2 magnetic susceptibility meter (Terraplus Inc.), which has a sensitivity of 1×10^{-6} SI and range from 0.001×10^{-3} SI to 1999.99×10^{-3} SI, along with the sample thickness by using a digimatic micrometer (Mitutoyo Corp.). The analytical error for the digimatic micrometer was 2 μm. I conducted 15 analyses on the center of each wafer for the measurement of magnetic susceptibility.

Results and Discussion

Results for HY lava show the peak of magnetic susceptibility. This peak could be because the sample thickness is beyond the range of the analytical depth for magnetic susceptibility. **This implies that the samples have boundary thickness to make the magnetic susceptibility constant.**

This study calls that boundary thickness as the effective thickness. The results indicate that the effective thickness for the HY lava is between 5 and 11 mm.

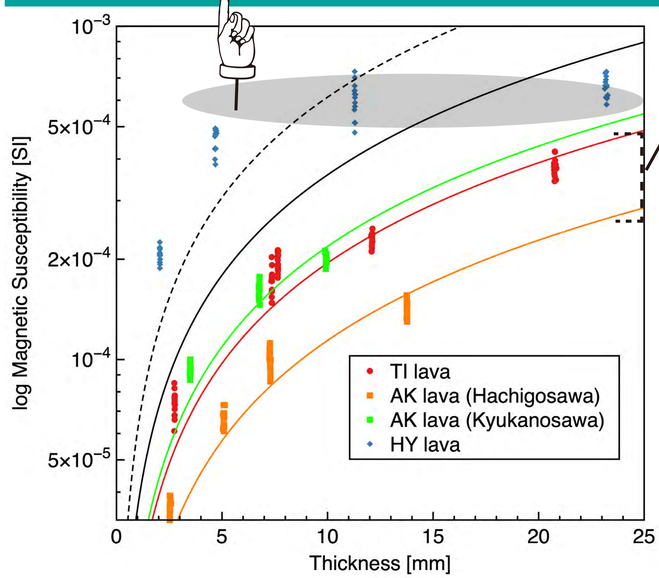

Fig. 3. Measurements of the thickness (mm) and magnetic susceptibility (SI) of the samples from the TI, AK, and HY lavas. The regression line for each analysis is also shown. The bold line corresponds to the regression line including all the measurement results, and the dashed line corresponds to the regression line including the results for the samples under 12-mm thickness in the HY lava.

Relation between magnetic susceptibility and rock texture

AK lava from the Hachigosawa and Kyukanosawa outcrops exhibited different trends for magnetic susceptibility.

The microlite number density (Nv number/m^3), in particular, was calculated from the number of crystals and the measured volume. The Nv values for Shirataki obsidian were 5.0×10^{13}–7.9×10^{13} /m^3 for the TI lava, 1.0×10^{14}–1.0×10^{15} /m^3 for the AK lava from the Hachigosawa outcrop, 1.1×10^{14}–1.8×10^{14} /m^3 for the AK lava from the Kyukanosawa outcrop, and 4.5×10^{13}–1.2×10^{14}/m^3 for the HY lava (Wada and Sano, 2011; Sano et al., 2015) and it is difficult to explain the difference in magnetic susceptibility based only on the difference in the number density. Oxide microlite in obsidian can vary in morphology, including acicular, euhedral and bead-like magnetite. Although further investigation is necessary to reveal the relationship between magnetic susceptibility and the texture of rocks, this heterogeneity in magnetite morphology could explain the different magnetic susceptibilities found in this study.

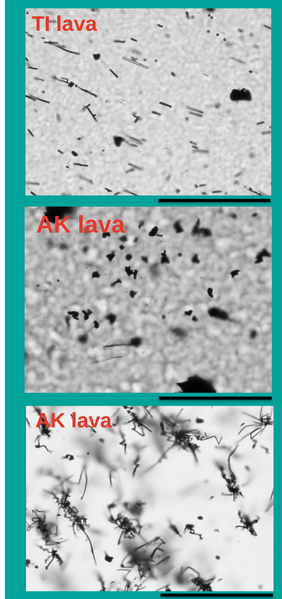

Fig. 3. Photomicrographs showing the oxide morphology in the obsidian from TI and AK lava flows. Scale bar is 100μm.

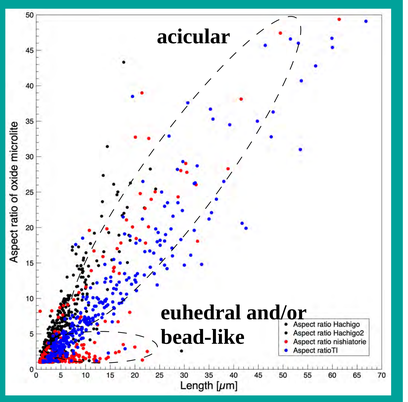

Fig. 4. Diagram showing the ralation between length and aspect ratio (length/width) of oxide microlite in obsidian.

Acknowledgments

I would like to thank Dr. Norihito Kawamura and Masato Sakiyama of University of Hyogo for their insightful comments and guidance on the measurement of magnetic susceptibility. I am indebted to the Shirataki-Geopark Promotion Department for assistance with the geological survey in the Shirataki area.

Imports and Outcrops: Characterizing the Baantu Obsidian Quarry, Wolaita, Ethiopia, Using Portable X-Ray Fluorescence

Benjamin D. Smith
University of Florida

INTRODUCTION

The Ethiopian branch of the East African Rift contains many obsidian sources (Negash *et al.* 2020) exploited as far back as 1.7 mya (Gallotti & Mussi 2015). It is an ideal region for studying long-term variation in technological organization and especially raw material procurement in contexts of evolutionary, demographic, and environmental change. At deeply stratified, well-dated sites like Mochena Borago rockshelter (Brandt et al 2012), archaeologists can examine even subtle shifts in obsidian procurement across broad time periods.

The Baantu obsidian quarry was the primary source of toolstone for Mochena Borago, although artifact types on the surface suggest quarrying and tool manufacture began much earlier than this.

Initial sourcing of the Mochena Borago obsidians identified some shifts in obsidian selection. However, a thorough survey of the quarry itself was needed to identify the geochemical fingerprint of the Baantu obsidian.

The quarry sits within a large area of eroded quaternary alluvium. Obsidian outcrops appear throughout, and obsidian artifacts cover the surface.

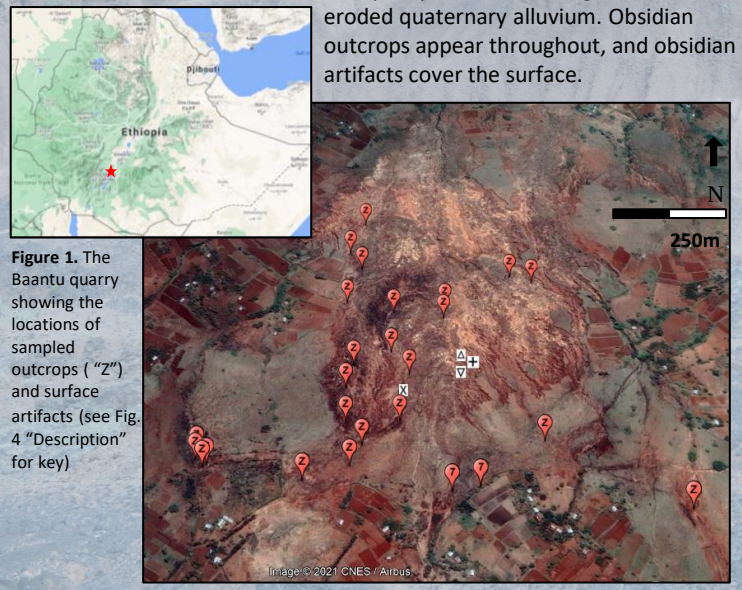

Figure 1. The Baantu quarry showing the locations of sampled outcrops ("Z") and surface artifacts (see Fig. 4 "Description" for key)

Outcrops and surface materials were likely exploited for toolstone. The goal of this project was to identify any variation in the Baantu obsidian outcrops and where possible identify imported obsidians.

MATERIALS & METHODS

Survey was made possible by the Wolaita Zonal Tourism offices, especially Ato Girma Dubusho. Our goal was to identify obsidian outcrops (Figs. 1, 2) relative to the surface material covering much of ~1km^2 Baantu surface area. Large flakes were struck from each outcrop. In some areas surface materials were collected along transects at regular intervals. This amounted to 32 sampled outcrops and 45 bags of lithic materials. Some volcanic tuffs and pottery were also collected

In the limited time available, I recorded 32 spectra at the Ethiopian Authority for Research and Conservation of Cultural Heritage (ARCCH) in Addis Ababa using a Bruker IIIeV Tracer + portable XRF spectrometer. These included:

- **25 obsidian outcrop flakes** (Fig. 2, see Fig. 1 for location).
- **6 obsidian artifacts** collected from the Baantu surface (Fig. 3).
- **1 obsidian artifact** from Mochena Borago.

Figure 3. Obsidian artifacts from Baantu surface a) aa large levallois core, b) a bifacial point, and c) grey/green obsidian.

Figure 2. Quarried obsidian outcrop at Baantu.

To maintain internal consistency, all XRF spectra were recorded on a single machine (Bruker IIIeV Tracer +, SN: K0437). It is equipped with a rhodium tube. The filter is composed of 1µm Ti, 12µm Al, 6µm Cu. It records MnKa1, FeKa1, ZnKa1, GaKa1, ThLa1, RbKa1, SrKa1, Y Ka1, ZrKa1, and NbKa1.

The machine was recalibrated on 11/6/2017 using the Bruker/MURR 40 standards, a Lucas-Tooth regression method.

Each sample was >3mm thick with a fresh break where possible, and large enough to cover the 3x4mm X-ray spot size. Spectra were recorded once for each sample using Bruker's accompanying software S1PXRF at 40kV in 180-second intervals.

RESULTS

K-Means cluster analysis (LMP) revealed five clusters within the 32 samples (Fig. 4). Obsidian outcrop flakes clustered together, and most surface artifacts fell within this range of variation.

Artifacts from cluster 1 likely represent another obsidian source and suggest that obsidian was being imported and quarried at Baantu.

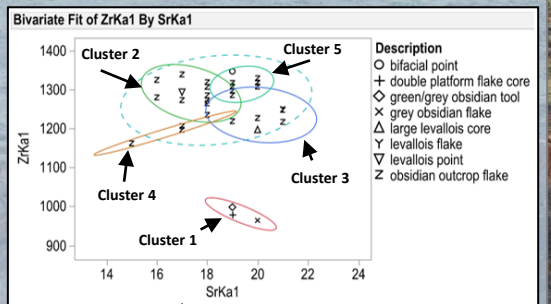

Cluster Means

Cluster	RbKa1	SrKa1	Y Ka1	ZrKa1	NbKa1
1	141	19	117	980	187
2	189	17	146	1290	255
3	180	20	140	1235	246
4	172	16	130	1188	237
5	191	19	150	1314	258

Figure 4. The largest 95% confidence ellipse is the grouping of all "outcrop" samples encompassing clusters 2-5, likely representing minor sub-groups among the outcrops. Cluster 1 likely represents a different source. Figures by L.R.M. Johnson

CONCLUSIONS AND FUTURE RESEARCH

The Baantu obsidian outcrops appear to cluster well together and this preliminary comparison suggests that they are distinguishable from imported obsidians. More data are needed to 1) evaluate cluster integrity, 2) identify possible sub-sources, and 3) assess the variety of imported obsidians represented on the surface.

Other obsidian sources in the region should also be sampled and compared to the Baantu outcrops using consistent calibration standards.

By identifying obsidians and reduction strategies at quarries and in well-dated archaeological sequences, archaeologists can address questions of temporal and spatial variation in obsidian procurement across major periods of evolutionary, environmental, and social change.

REFERENCES:

Brandt, S. A., Fisher, E. C., Hildebrand, E. A., Vogelsang, R., Ambrose, S. H., Lesur, J., & Wang, H. (2012). Early MIS 3 occupation of Mochena Borago Rockshelter, Southwest Ethiopian Highlands: implications for Late Pleistocene archaeology, paleoenvironments and modern human dispersals. *Quaternary International*, 274, 38-54.

Gallotti R, Mussi M (2015) The Unknown Oldowan: ~1.7-Million-Year-Old Standardized Obsidian Small Tools from Garba IV, Melka Kunture, Ethiopia. *PLoS ONE* 10 (12): e0145101.

Negash, A., Nash, B. P., & Brown, F. H. (2020). An initial survey of the composition of Ethiopian obsidian. *Journal of African Earth Sciences*, 172, 103977.